HHS Public Access

Author manuscript

*Kidney Int*. Author manuscript; available in PMC 2014 November 01.

Published in final edited form as:

*Kidney Int*. 2014 May ; 85(5): 1225–1237. doi:10.1038/ki.2013.422.

# Subfractionation, characterization and in-depth proteomic analysis of glomerular membrane vesicles in human urine

**Marie C. Hogan**[1,*], **Kenneth L. Johnson**[2], **Roman M. Zenka**[2], **M. Cristine Charlesworth**[2], **Benjamin J. Madden**[2], **Doug W. Mahoney**[3], **Ann L. Oberg**[3], **Bing Q. Huang**[4], **Lisa L. Nesbitt**[1], **Jason L. Bakeberg**[1], **H. Robert Bergen III**[2], and **Christopher J. Ward**[1]

[1]Division of Nephrology & Hypertension, Department of Internal Medicine, Mayo Clinic, Rochester, MN

[2]Mayo Clinic Proteomics Core, Medical Sciences Building, Mayo Clinic, Rochester, MN

[3]Biomedical Statistics and Informatics. Mayo Clinic, Rochester, MN

[4]Mayo Electron Microscopy Core Laboratory, Mayo Clinic, Rochester, MN55905

## Abstract

Urinary exosome-like vesicles (ELVs) are a heterogenous mixture (diameter 40–200nm) containing vesicles shed from all segments of the nephron including glomerular podocytes. Contamination with Tamm Horsfall protein (THP) oligomers has hampered their isolation and proteomic analysis. Here we improved ELV isolation protocols employing density centrifugation to remove THP and albumin, and isolated a glomerular membranous vesicle (GMV) enriched subfraction from 7 individuals identifying 1830 proteins and in 3 patients with glomerular disease identifying 5657 unique proteins. The GMV fraction was composed of podocin/podocalyxin positive irregularly shaped membranous vesicles and podocin/podocalyxin negative classical exosomes. Ingenuity pathway analysis identified integrin, actin cytoskeleton and RhoGDI signaling in the top three canonical represented signaling pathways and 19 other proteins associated with inherited glomerular diseases. The GMVs are of podocyte origin and the density gradient technique allowed isolation in a reproducible manner. We show many nephrotic syndrome proteins, proteases and complement proteins involved in glomerular disease are in GMVs and some were shed in the disease state (nephrin, TRPC6 and INF2 and PLA2R). We calculated sample sizes required to identify new glomerular disease biomarkers, expand the ELV proteome and provide a reference proteome in a database that may prove useful in the search for biomarkers of glomerular disease.

### Keywords

Exosome; proteomics; podocyte; glomerular disease; Integrin; actin cytoskeleton; Rho GDI. Q-Exactive mass spectrometer



*Corresponding author: hogan.marie@mayo.edu.

Urinary microparticles known as exosome-like vesicles (ELVs) are derived from two distinct cellular sources, the multivesicular body (MVB) (true exosomes) and apical cell membrane (membrane vesicles).[1–6] They are shed from the entire genitourinary epithelium (kidney, urothelium, prostate, bladder), and an important subpopulation appears to originate from the glomerulus. These could be a rich source of biomarkers permitting non-invasive assessment of glomerular health.[5] Bulk ELV subfractionation has not been possible due to large amounts of Tamm-Horsfall protein (THP) in urine, as under physiological conditions, THP oligomerizes into long double helical strings.[7] In centrifugation-based protocols it tends to precipitate under high "g" forming a gel which traps and sequesters ELVs.[8] A variety of techniques have been used to reduce the amount of THP in ELV preparations-the most important being use of dithiothreitol (DTT) to reduce the disulfide bonds in the THP ZP (Zona pellucida) domains, abolishing its ability to oligomerize, but even under these conditions[4] significant amounts of reduced THP still precipitate upon ultracentrifugation, and dominates the proteomic landscape of urine ELVs especially in the range 80–110kDa.[4,8] Another approach is to generate an exclusion list of THP MS1 peptide masses, which can be used to exclude THP peptides from further analysis in the MS2 dimension (which generates sequence data).[9] However, this runs the risk of excluding peptides from non-THP proteins, although it tends to uncover more peptides than it loses.[9] Our $D_2O$ 5–30% sucrose gradient method pellets the vast majority of the THP to the bottom of the ultracentrifuge tube (see figures 2b and d Hogan et al 2009), with ELV subfractions banding at different specific densities[10].

In prior studies we identified ELV subfractions enriched for specific kidney disease proteins, including a fraction containing the major polycystic kidney disease proteins polycystin 1,2 and fibrocystin (all thought to be of tubular origin), which permitted examination of the post-translational processing of these proteins and provided the first *in vivo* evidence of polycystin 1 GPS domain cleavage.[11,10, 12] We and others have also identified podocin and several other glomerular disease proteins in ELVs.[4, 13, 141516] A comprehensive analysis of the shed glomerular membrane vesicle (GMV) proteome together with measurement of intra individual variability is required before attempts are made to study the GMV proteome in preparation for biomarker discovery studies.

Utilizing $D_2O$ 5–30% sucrose gradient density centrifugation we have now focused our isolation method to study the GMV sub-fraction. Antibodies to podocalyxin and podocin, regarded as major podocyte surface antigens, (the visceral epithelial cells of Bowman's capsule) were used to study their morphology.[17, 18] We performed a comprehensive proteomic analysis of this subfraction enriched in GMVs (apical membrane vesicles) and then assessed the overlap of our GMV proteome with the published glomerular tissue and urine exosome proteomes.[19] We studied the post-translational processing of a number of known glomerular disease proteins for the first time *in vivo* and provide these data in a searchable database.

## Results

### Clinical characteristics of participants

Urine was collected from seven healthy volunteers, four males and three females, aged 17 to 34 years (mean age 27, average albumin /creatinine ratio 1.63mg/g (0–5.76mg/g) (IRB #09-003355). Normal random urine albumin excretion <17 mg/g creatinine (males) and <25 mg/g creatinine (females)). None of the volunteers were hypertensive and all were non-smokers. Average serum creatinine was 0.95±.07mg/dL. Urine was obtained from three adults with glomerular disease (IRB#07-004128) (Table 1).

### Pre-Fractionation of GMVs

We obtained 270ml of fresh urine from each of seven individuals and centrifuged them at low g-force to remove cells and debris, then ultracentrifuged them at 150,000g for 1hour to pellet a mixture of THP and ELVs, termed “crude exosomes”. THP was further removed from the ELV fractions by centrifugation on a 5–30% sucrose gradient in $D_2O$ (200,000g × 24 hours). We found three distinct bands of visible ELVs scattering light when the 5–30% sucrose $D_2O$ gradient was illuminated along its long axis and which we could reproducibly and accurately collect (figure 1A).[20] We designated the three bands as A, B and C; A being the lightest RI- $\eta$=1.3436 sd+/−0.00124, B the band of intermediate density band (PKD-ELVs) RI $\eta$=1.3539 sd+/−0.000831 and C the highest density (GMVs) RI $\eta$= 1.3625 sd+/−0.000911.

### Characterization of GMVs by western blot and electron microscopy

On transmission electron microscopy (TEM) of the purified ELV fractions, fraction A was characterized by the presence of large ~200nm ELVs, which have a classical "punched-out soccer ball" appearance (median diameter 93.0nm (IQR 75.3–128.8nm) with a right skewed distribution), fraction B contained mainly classical ELVs (median diameter 79.4nm (IQR 54.6—103.9nm),and GMV (membrane particles) were most abundant in fraction C (median diameter 72.1nm (IQR 50.2–93.8nm), left skew). In fraction C there were smaller membrane fragments that lacked the distinct appearance of classical ELVs, stained poorly with uranyl acetate and were podocin/ podocalyxin positive (termed GMVs). GMVs accounted for 23.3% of all particulate content in fraction B and 44.7% of particulate content in the fraction C grids surveyed) with the remainder in each being “classical” ELVs which did not stain for podocin/podocalyxin (figure 1C; figure 2A). Median classical exosome diameter was 91.4nm (IQR 76.9–109.2nm) compared with GMV diameter of 45.8nm (IQR 35.9–56.1nm) (p-value < $2e^{-16}$, Wilcoxon test) in fraction C (figures 2A & B). Using KS permutation testing, we also observed a clear shift indicating a difference in the diameters of two particle types ($p<0.0001$) (Supplemental figure 1).

These differences were also reflected in Western blots of the three fractions, Fraction B being enriched for polycystin-1, more than fraction A or C; fraction C being podocalyxin positive with only weak detection of polycystin-1 (figure 3A). Thus, while this method isolates a heterogenous population of vesicles (albeit a not completely pure GMV fraction), it permits a first time assessment of their morphology and peptide level proteomic data at peptide depth not previously accessible (supplemental table 2A).

### Effective removal of contaminating THP

Virtually all THP migrated to the pellet at the bottom of the ultracentrifuge tube leaving the banded ELV fractions clear of THP. This was seen when we analyzed ELV fraction C by SDS-PAGE analysis. Fraction C protein ran as a multitude of bands whereas the starting material-"crude exosomes" was dominated by a large band of THP no longer visible in the purified Fraction C ELVs (figure 3B compared **to** 3C, 3D & 3E). This was also reflected in the proteomic analysis of gel slice D (70–90kDa, THP Mwt=85kDa) in fraction C where THP was no longer the most abundant protein (by either spectral counting or sequence coverage).

### Proteome Characterization of GMVs

We separated 30μg of ELV fraction B (PKD-ELVs) and C (GMVs) material from each individual on a 4–12% SDS-PAGE gel and then sliced it into 10 horizontal gel band segments (A–J) for proteomic analysis by LC-MS/MS (figure 3B), generating 140 individual samples. We also pooled equal protein amounts of the seven fraction C samples (GMV fraction) and ran this on both a 10–14% and a 5% SDS gels; each lane was then cut into 45 and 36 slices respectively (figures 3D, 3E). Each slice was analyzed by LC-MS/MS. Data from both LC-MS/MS experiments was searched using a combination of Mascot, Sequest and X!Tandem (figure 3F).[21, 22] A total of 2190 proteins were identified by LC-MS/MS analysis from the ELVs from both sucrose gradient fractions B and C combining all methodologies (figures 3F, 4A, 4C). A total of 1830 proteins were identified in the GMVs (fraction C) combining all methodologies (figure 4B). The glomerular origin was confirmed by presence of podocin in fraction C but not in B (figure 2C; supplemental table 1). We found 1106 proteins were common to all seven individuals of fraction C (supplemental figure 2). We also found 27% (599/2190) proteins were present in the glomerular tissue proteome, implying that a specific subfraction of glomerular proteins are secreted (figure 5A).[19]

### Hereditary glomerular disease proteins

We identified many hereditary glomerular disease proteins, the majority with greater peptide number than previously reported in other exosome studies (table 2, supplemental tables 1 and 2).[4, 13] These included podocin, alpha-actinin-4, CD2-associated protein, myosin-9, myosin 1E, cdc42, CD151, Rho GDP-dissociation inhibitor 1, integrin alpha 3 and cubilin. Podocin (exclusively seen in gel slice F;~40–55 kDa range across all seven controls) is reported to have two isoforms- 42 and 34 kDa, the latter characterized by absence of amino acids 179–246 (Uniprot.org). The peptides identified were outside of that range, and therefore while the MS data could not distinguish which isoform was present, our molecular weight data from the 1D-SDS gel suggests isoform 1 was the secreted GMV form (supplemental table 2). Several proteins mutated in atypical hemolytic uremic syndrome (complement C3, C4B and factor B; table 2) were also present.[23]

### Proteins involved in glomerular biology

Podocalyxin (59 kDa mass by amino acid sequence) has multiple O-linked and N-linked sugar modifications and coats podocyte secondary foot processes.[17, 24] Consistent with these

reports, we identified its peptides only occurring C terminal to the heavily glycosylated region (figure 2C), with highest abundance in gel slices A, B, and C (supplemental table 3). A number of other proteins implicated in glomerular biology were identified (table 3).

## Large proteins & Proteases

Several very large proteins were distinguished by visible Coomassie bands (figure 3E) in the high MW GeLC experiments: IgGFc-binding protein (a gigantic protein with 5,405 amino acids with a nonimal unprocessed molecular mass of 572KDa were present (38 peptides; band 28), megalin, the Heymann nephritis antigen (low-density lipoprotein receptor-related protein 2 mutated in Donnai-Barrow and facioocculoacousticorenal syndrome, associated with proteinuria) a 522kDa protein (most abundant protein slice 8), maltase (slices 8 &13) and ACE, α2 macroglobulin & ACE2 (in slice 23) and aminopeptidase N (slice 29). Peptide coverage of both ACE and ACE2 was higher using our methodology than in prior studies (table 2; Supplemental table 1); ACE, a membrane-bound enzyme is anchored by its hydrophobic carboxyl-terminal segment and is also a circulating protein in body fluids and could indicate their secretion from podocytes could be through shedding on GMVs, as opposed to secretion following enzymatic cleavage.[13] Several lysosomal proteinases anticipated to exist in the classical MVB-derived exosomes but not on GMVs, were detected in fraction C (cathepsins A, B, C, D and H) and could maintain some proteolytic activity in urine.[25] The presence of others- (cathepsin G-the first observation that it could be shed from the podocyte; 3 peptides 11% coverage; gel slice J; all 7 controls), neutrophil elastase and myeloperoxidase suggests these cationic autoantigens may be disposed of through GMVs.

## Pathway Analysis

Ingenuity pathway analysis (Supplemental table 3) identified the integrin signaling (−log p value: 26.2), actin cytoskeletal (−log p value: 23.55) and Rho GDI (involved in membrane ruffling) (−log p value: 23.1) were the signaling networks identified with the highest statistical significance in fraction C. Reactome pathway analysis (www.Reactome.org) also identified the statistically most over- represented pathway was membrane trafficking (REACT_11123;) with products of 75 of 192 genes in this pathway identified (un-adjusted probability of seeing N or more genes in this event by chance was −log p value 27). (Supplemental table 3).

## High resolution mass spectrometry in individuals with glomerular disease

Using identical conditions we isolated GMV subfractions from three individuals with glomerular disease (2 membranous nephropathy cases and another individual with $IgG_3$ membranoproliferative glomerulonephritis (figure 6). The initial ultracentrifugation spin precipitated THP as usual (figure 6A)but with only small amounts of albumin retained in the pellet (figure 6C; compare control with cases) implying that it is retained in solution under these conditions with negligible albumin in the respective pellets following the $D_2O$ sucrose gradient step (figure 6C) step. Using the same gel slice technique we identified a total of 5657 proteins using the Q-Exactive™ mass spectrometer (Supplemental table 4). GMV morphology was identical to the healthy control samples but importantly we detected the all the nephrotic syndrome proteins and several others not detected in the healthy controls (e.g.

nephrin, TRPC6, INF2, IQGAP1; and the idiopathic membranous nephropathy target autoantigen $PLA_2R$; Supplemental table 4).

## Discussion

We provide an isolation protocol for purification of glomerular membrane vesicles, describe their morphology and catalog their proteome in healthy controls and individuals with nephrotic syndrome/glomerular disease. We expand the known urine exosome proteome and show how it overlaps with the glomerular tissue proteome. Our first technique, an analysis of 7 independent samples, identified 1720 proteins in the fraction most abundant in GMVs and the second approach using pooled samples (Gel C) contributing an additional 110 proteins. At least 387 proteins not hitherto observed in ELVs (figure 5B) include the proteinase 3 receptor, CD177.[26] Furthermore, we identified 497 proteins not detected in the largest urine exosome proteomic study to date.[15] We then studied fraction C samples from individuals with glomerular disease with proteinuria using high resolution mass spectroscopy confirming the isolation method is valid in proteinuric states and identified 5657 proteins, supplying the largest urine based proteome reported to date in glomerular disease (supplemental table 4). The much larger number of proteins identified can be accounted for by the new high performance instrument a hybrid quadrupole-orbitrap.[27] Our databases will be for useful for isoform identification and in selection of suitable peptides (also supplied) for quantitative proteomic approaches in candidate biomarker proteins (Supplemental tables 2 & 4).

Transmission electron microscopy (TEM) delineated the morphology of the podocin/podocalyxin positive GMVs as irregular membrane fragments (average diameter 62.5nm). Fraction C also contains classical exosomes, with their “punched out soccer ball” appearance, negative for podocin/podocalyxin. Podocalyxin and podocin are found exclusively on podocyte apical foot process surfaces (i.e. directly adjacent to the urinary space) implying that GMVs shed from the visceral aspect of the podocyte into urine.[28] Hara *et al*. also described shedding vesicles termed podocyte membrane vesicles which are CD24/CD63 negative (i.e. unlikely to be of MVB origin).[29] and others showed podocalyxin -GFP exits by a (<100nM diameter) vesicular pathway from the leading edge of the cell and speculated these vesicles contain macromolecular complexes of other glomerular proteins.[30] Network analysis of the fraction C proteome shows that actin cytoskeletal pathway scored highly, leading us to propose that GMVs are generated via interaction between the cytoskeleton and the membrane, in short by membrane ruffling (Supplemental table 3). Therefore, available data on GMVs strongly suggests a podocyte membrane origin.

GMVs contain proteins involved in genetic causes of glomerulonephritis and acquired glomerulopathies (tables 1 & 2). Nephrin, TRPC6 and INF2 were detected in all proteinuric cases but not in normal controls.. Nephrin, a slit diaphragm protein is tethered to the membrane as a stable structural protein only dislodged in disease; TRPC6 an ion channel is also stably tethered to the podocyte cell membrane may also be in a stable complex, perhaps with nephrin as also may be the case for INF2 and shed in GMVs.[3132–34] The FSGS protein, CD2AP, a dynamic and promiscuous adapter protein was abundant and is known to bridge the actin cytoskeleton with membrane proteins (table 2)- further supporting the idea of a

podocyte membrane origin for GMVs. The target autoantigen M-type phospholipase $A_2$ receptor ($PLA_2R$) seen in patients with idiopathic membranous nephropathy was detected in all three cases but not in controls and as this is the first analysis of GMVs in individuals with membranous nephropathy these findings will need to be followed up in other cases to understand their significance[35]. WT1 was not seen in either group likely explained by its location as a nuclear transcription factor protein[36,37]

ANCA antigens implicated in pauciimmune glomerulonephritis, human leucocyte (neutrophil) elastase, myeloperoxidase (both in fraction C) and proteinase 3 (fraction B) were present (Supplemental table 1). These cationic azurophil granule proteins are exclusively contained in cells of myeloid lineage-neutrophils and monocytes. We theorize that when circulating neutrophils degranulate or become senescent, cationic proteins are released into the blood and some of these are delivered to the polyanionic glomerular basement membrane where they are detected and removed by the podocyte, then shed on GMVs into the urine space.[38–42] This may protect the polyanionic membrane from proteolytic assault and prevent accumulation of autoantigenic neoantigens on the glomerular membrane. Therefore, membrane-bound neutrophil derived proteinases may be candidate biomarkers in granulomatosis with polyangiitis (e.g. ANCA vasculitis). The presence of complement components (C3b and C4b) and complement inhibitors such as CD59, together with large proteins involved in immunoglobulin binding (IgGFc-binding protein) suggests podocytes participate in clearing immune complexes, some of which appear in urine bound to GMVs.

This study utilizes and refines the 5–30% sucrose heavy water continuous gradient first described in our previous study to identify a fraction of ELVs rich in membrane fragments from the glomerular podocyte (GMVs).[10] Others have used $D_2O$ gradient ultracentrifugation since our 2009 report but with their double- cushion method (and similar stringent criteria for protein identification they identified only 378 proteins.[16] The success of our study depended on two other significant technical advancements (1) our label free-method provides non-denatured protein free of THP and albumin with a reproducible proteome (Supplemental figure 2) as characterized by the number of proteins identified[16, 43, 44] (2) powerful 1D separation methods supply information about molecular mass of the parent protein, which in turn can be used to guide research into differential splicing, glycosylation and proteolytic cleavage of interesting proteins as opposed to proteomics studies where fractionation occurs after proteolysis. Though our method is not practical in a high throughput clinical setting, it is suitable for ELV/GMV biomarker discovery work.[15,40,41] Promising candidates could then be validated with multiple reaction monitoring permitting directed analysis of target biomarker peptides using higher throughput filter-based techniques for enrichment of urine exosomes.[45]

We performed a simulation using spectral intensity data using three possible scenarios using our data and calculated the number of individuals in a disease and control group required for an 80% power and 5% FDR to detect a ≥2× difference in protein abundance. Different proteins showed different degrees of variability using intensity (Supplemental table 2, Supplemental figure 3). Twenty individuals per group (disease versus normal controls)

would permit detection of a ≥2× difference in the ≤5% most differentially regulated proteins.

In conclusion, with improvements in our ELV isolation and proteomics methods, combined with the ability to remove THP and albumin from urine, we predict the ability to isolate urinary GMVs will be useful for the study of proteins involved in the pathogenesis of human glomerular disease.

## Methods

### Enrollees and clinical evaluation

Mayo IRB approved this study. Consent was obtained for urine collection from healthy normotensive individuals <40yrs with normal renal function, no hypertension & absence of microalbuminuria and three individuals with glomerular disease (#1; #2; #3). Urine albumin was measured by immunoturbidimetry utilizing antibody to human albumin in an automated immunoprecipitin analysis system. (Package insert: Tina-Quant Albumin Reagents Kit for urinary albumin, Roche Diagnostics, Indianapolis, IN, March 2007). Creatinine was measured by the enzymatic method (Roche Diagnostics, Indianapolis IN).

### Density centrifugation

Two hundred and seventy milliliters of first or 2nd AM void urines which was spun at low speed 4000g × 15 minutes in a chilled centrifuge (at 4°C), (as opposed to the 17,000g used by Pisitkun, as this was sufficient to clear cells and debris without reducing the yield of ELVs) then supernatant was sieved on a 80μm porous nylon filtration membrane (www.sefar.com; 12× 12 in; Item 7050-1220-000-20) to remove particulate matter and supernatant was then ultracentrifuged at 4°C at 150,000g ×1 hr. ELV pellets were resuspended in 0.25M sucrose 20mM MES pH6.0 with protease inhibitor (Complete no EDTA; Roche®) & centrifuged × 24h @200,000g on 5–30% sucrose $D_2O$ gradient at 4°C (figures 1 & 2) and then fractionated according to the visible 3 bands by refractive index; zone A the lowest density $\eta$=1.3436 SD+/−0.00124, intermediate density B $\eta$=1.3539 SD+/−0.000831 & highest density C $\eta$= 1.3625 SD+/− 0.000911[4]. These were harvested using a Biocomp gradient station (Biocomp Canada; www.biocompinstruments.com) and pelleted overnight at 100,000g in PBS/Complete at 4°C no EDTA. Exosome gradient fractions from three patients with history of documented nephrotic syndrome and biopsy proven glomerular disease (~150–250ml raw urine) were handled in the same way.

### Gel Analysis

Thirty micrograms of protein (pooled podocin-rich fraction- Zone C) of each individual was separated with 1D PAGE 4–12% MOPS % then divided into 10 gel slice sections using prominent protein bands common to all samples as markers and spiked-in proteins of known mass. For each sucrose gradient fraction B and C we pooled equal amounts of protein from 7 (B) and 7 (C) normal human subject samples. We did not run fraction A samples due to cost. The pellet from each nephrotic patient was air-dried, and re solubilized in 20 ul of Novex sample buffer + 50mM TCEP; 2 ul was ran on a test gel to determine the relative amount of protein and possible albumin contamination. The remainder of each sample was ran on a 4–

12% Novex minigel and 8–10 sections per gel cut out for MS analysis, with the goal of identifying as many proteins as possible in the three patient samples.

### One Dimensional Gel separation GeLC-MS

For optimal protein separation, we ran 2 gels on each pooled sample optimized for high molecular weight (HMW) 5% gel (SGE0610-01) and low molecular weight LMW – (10.5–14% gel) (SGE0610-02) protein analysis. For the LMW gel (SGE0610-02): 45 bands from the LMW gel were cut out and submitted for MS "B" lane = sucrose gradient fraction B - pooled normal samples "C" lane = sucrose gradient fraction C - pooled normal samples. For the HMW gel (SGE0610-01): 36 bands from "C" sucrose gradient fraction lane were cut out and submitted for MS (figures 3D & E).

### Antibodies

We used the following antibodies: podocin (Sigma; (H-130) sc-21009 (200 μg/ml), polycystin 1 (7E12 monoclonal AB; Santa Cruz) and human specific podocalyxin (3D3.28, Santa Cruz; gift from Drs. Kershaw and Wiggins).

### Western Blot

Isolated ELV subfractions were subjected to immunoblot as described previously. Polycystin 1 antibody was used at 1: 1000 concentration, podocalyxin was used a 1;1,000 concentration (gift Drs. Kershaw and Wiggins, U Michigan). All blots were performed on nitrocellulose membranes and blocked with 5% non-fat milk.

## Supplemental Methods

### Electron microscopy

Podocin and podocalyxin antibodies were labeled with 15 nm protein A-gold on zone C ELVs from 6 normal controls (3 males and 3 females). Anti-polycystin 1 (7e12) and podocalyxin (3D3) was applied to two fraction C samples. Double staining was not possible due to the shared IgG1 isotype for both podocalyxin and polycystin 1 antibodies. All negative controls used had no primary antibody. Immunoelectron microscopy was performed as described previously.[10] The concentrated solution of exosome fractions prepared as described above was mixed 1:1 with 4% paraformaldehyde in phosphate-buffer (pH 7.2) and then applied to 200-mesh Formvar-carbon coated nickel grids. The grid was stained with 2% uranyl acetate, pH 7, and embedded with 2% methylcellulose/0.4% uranyl acetate, pH 4. After drying, grids were examined with a transmission electron microscope (JEOL ExII).Particle diameter measurements were performed by one observer (JB) using Image J (NIH).

### Statistical analyses

For particle diameter analysis the data was trimmed removing objects with diameters >400nm. Distinguishing criteria for GMVs (done by CJW) were a non-clumped isolated membranous particle with the presence of 3 or more podocalyxin positive gold versus non-staining ELVs within the same image field. The maximum diameter of each vesicle was measured by TEM at 80,000× magnification and a total of 705 vesicles were scored as

classical exosomes (n=390) or glomerular membrane vesicles (n=315) in fraction C. Total for fraction B were 437 particles, across three different subjects. Since data was skewed to the left we utilized a non-parametric Wilcoxon test. Results are expressed as median and interquartile range. Comparison of distribution of vesicle diameters between classical and irregular shaped vesicles was also performed using Kolmogorov-Smirnov test (KS). Since the data consisted of 3 subjects with paired sampling of vesicle sizes, the test of significance for the KS test had to be modified to account for within subject correlation. To achieve the appropriate statistical significance, 5000 random permutations of Kolmogorov-Smirnov test statistic per subject were calculated to estimate the null-distribution. The observed Kolmogorov-Smirnov test per individual was then compared to null-distribution as well as averaged across subjects to perform an overall test. This overall test of significance used per-subject weights proportional to the total variance (sigma_i/sum(sigma_i)). For pathway analysis in the normal controls a list of human UniProt/SwissProt ID identified in Fraction C was used as an input to Ingenuity Pathway Analysis software (Ingenuity® Systems, www.ingenuity.com Redwood City, CA). As result, we identified canonical pathways enriched (p-value < $10^{-10}$) by proteins from the input list.

## Database Searching

Tandem mass spectra were extracted and charge state deconvoluted by extract_msn v.3 (parameters: -Z -V -MP100.00 -EA100 -S1 -I10 -G1). Deisotoping was not performed. All MS/MS samples were analyzed using Mascot (Matrix Science, London, UK; version Mascot), Sequest (Thermo Fisher Scientific, San Jose, CA, USA; version 27, rev. 12) and X! Tandem (The GPM, thegpm.org; version 2006.09.15.3). All search engines were set up to search SwissProt (rel. 2010_05, filtered _HUMAN proteins, 20283 entries + 20283 reversed) assuming digestion by trypsin. Mascot and X! Tandem were searched with a fragment ion mass tolerance of 0.60 Da and a parent ion tolerance of 20 PPM. Sequest was searched with a fragment ion mass tolerance of 0.60 Da and a parent ion tolerance of 0.081 Da. Oxidation of methionine, iodoacetamide derivative of cysteine and acrylamide adduct of cysteine were specified in Mascot, Sequest and X! Tandem as variable modifications.

## Criteria For Protein Identification

Scaffold (version Scaffold_2_06_01, Proteome Software Inc., Portland, OR) was used to validate MS/MS based peptide and protein identifications. Protein identifications were accepted if they could be established at greater than 95% probability and contained at least 2 identified peptides.[46] Proteins that contained similar peptides and could not be differentiated based on MS/MS analysis alone were grouped to satisfy the principles of parsimony. Uniprot IDs were generated via SWIFT using Sequest, Mascot, and X!Tandem, validated via Scaffold and filtered using a 1% false discovery rate (FDR)[47]. FDR is defined as the “expected” proportion of incorrect assignments among the accepted assignments at the global level[48]. Venn diagrams from ID'ed protein lists required a minimum of 2 unique peptides, Scaffold 95% probability at the peptide level, 95% probability at the protein level, and filtered using precursor mass tolerance to achieve 1% FDR. Protein export files were created and exported into Excel using the filtering conditions highlighted above. Additionally, trypsin, the 3 spike-in protein internal standards, and any reversed sequence protein hits (decoy hits) were removed from the export list that was used for generation of

the Venn diagrams. Fraction B and C proteins were compared (supplemental table 1, figures 4C & 5). These would include proteins identified by only peptide with Elucidator® (Rosetta Biosoftware) (Mascot search only) that passed Peptide Teller and Protein Teller filtering at the approx 1% FDR. Shared protein output of two search engine analyses (SWIFT: 2 peptides identified for each protein detected and 1% FDR) with Elucidator® (with minimum of 2 peptide requirement) of Fraction C and Gel C data revealed 1500 shared proteins (supplemental table 2). This approach removed Elucidator® single peptide hits (from a Mascot search only) that passed Peptide Teller and Protein Teller filtering at the approx. 1% FDR. This dataset was used to characterize inter-individual variability and we used Excel pivot tables to combine proteins from 7 patients and establish a protein "heat map" (Table S2D). For comparisons to other databases, Perl scripts were used to translate their protein lists. Some proteins could not be translated (not mapped) because they referred to proteins no longer listed in Uniprot.

### 1-Dimensional PAGE Gels

Three exogenous proteins were added to each sample prior to SDS-PAGE separation: β-galactosidase from *E. coli*, (BGAL_ECOLI), ovalbumin (OVAL_CHICK), and bovine β-lactoglobulin (LACB_BOVIN) (Sigma Chemical, St. Louis, MO). 200fmol of each protein was added to each lane.

### In-Gel Digestion of Gel Sections

The 1-D SDS-PAGE gel lane from each sample was excised into 10 sections using prominent bands present in all lanes to demarcate each section (figure 3B). Each gel section sample was further cut into approximately 1 $mm^3$ pieces and stored at −80° C until digestion. Gel samples were first hydrated with 150 mM Tris, pH 8.3, were de-stained using 50% isopropanol in 150 mM Tris, pH 8.3, dehydrated with isopropanol, followed by reduction with 40 mM dithiothreitol (DTT) for 30 min. at 55° C and alkylation with iodoacetamide (50 mM, 30 min., room temperature, dark). Gel pieces were dehydrated between reduction and alkylation steps with isopropanol to remove excess reagent. Thirty μL of 4 ng/μL sequencing grade trypsin (Promega, Madison, WI) dissolved in 20 mM Tris, pH 8.3 containing 0.0002% Zwittergent 3–16 detergent (CalBiochem, San Diego CA) was added to dehydrated gel pieces. After initial rehydration, an additional 20 μL of 20 mM Tris, pH 8.3 was added and samples were digested overnight at 37°C. Digested peptides were sequentially extracted with 2% TFA, followed by two aliquots of acetonitrile, each step for 30 minutes at ambient temperature. The combined extracts for each sample were briefly frozen at −80°C prior to evaporation to dryness on a vacuum centrifuge. Dried tryptic peptide extracts were stored frozen at −80°C until analysis by mass spectrometry. Samples from each gel section were reconstituted in water containing 0.1% TFA, 0.2 % formic acid, and 0.002% Zwittergent 3–16 that also contained 2fmol/μL angiotensin I, to monitor instrument performance for each injection.

### LC-MS/MS

For the normal controls mass spectrometry (MS) data was acquired using nano scale liquid chromatography coupled with high mass accuracy mass spectrometry and data-dependent

tandem mass spectrometry (nLC-MS/MS). An Eksigent model nanoLC-2D (Eksigent, Dublin, CA), interfaced with an LTQ-Orbitrap (Thermo Fisher Scientific, Bremen, Germany) was used to perform 75 minute separations (3–40%B in 50 min.) on a 25cm long by 75 micrometer (μm) inside diameter spray tip packed with Magic $C_{18}$AQ (3μm particles, 200 Å pore size, Michrom BioResources, Auburn, CA). Samples were pre-concentrated on an OptiPak 0.25 uL trap packed with Magic C8, (5 μm, 200 Å) (Optimize Technologies) at 15 μL/min using an Eksigent AS1 autosampler, injection volumes of 5–20 μL, and an aqueous loading buffer of 0.05% TFA and 0.15% formic acid. MS data was collected in a data-dependent manner by acquiring an Orbitrap survey scan (60,000 resolving power at m/z 400 FWHM, AGC target of $1 \times 10^6$ ions), and tandem MS (MS/MS) experiments in the linear ion trap (LTQ) on the five most abundant doubly or triply charged precursor ions from each survey scan (31% NCE, isolation width=2.2, $8 \times 10^3$ ions, 80 ms maximum ionization time). Precursor ions were excluded for 45 seconds after selection for an MS/MS experiment.

Samples were run in blocks by gel section, using a different order within each gel section to minimize run order bias. Each sample run was followed by a blank run using a shorter LC gradient. Each sample block was preceded and followed by QA/QC samples consisting of a commercial tryptic digest of yeast enolase (Waters Corp.) to check sensitivity and chromatographic performance, and a tryptic digest of yeast lysate to track the number of proteins identified.

### Relative Protein Quantification

Relative protein quantification for the seven subjects was performed on the Orbitrap survey scan (MS1) data using the Elucidator software package (Rosetta Biosoftware, Seattle, WA)[21, 22] Elucidator aligns, measures abundance, and scores mass spectral features in each sample based upon their chromatographic and m/z profiles. Features surpassing minimum peak m/z scores of 0.9, peak time scores of 0.8, and LC peak widths of 0.125 minute were carried forward in the workflow of assigning amino acid sequence and comparing their relative abundance.

Peptide sequences were assigned to MS/MS spectra using the MASCOT database search engine (Ver. 2.2.04, www.matrixscience.com) and searched against the human subset of the Uniprot/Swiss Prot database. Validation of the database search results was done using the Elucidator implementation of Peptide Prophet and Protein Prophet algorithms[46, 49] with an estimated false discovery rate of 1% estimated by the algorithms, while using reversed sequence protein entries appended to the database as decoys.[46,47,50] Validated peptides were annotated to their molecular signals across the aligned data from each sample.

### Protein identification via in gel trypsin digest and nano LC-MS/MS with high resolution mass spectrometry

For the glomerular disease samples the SDS-PAGE gel bands were prepared for mass spectrometry analysis using the following procedures. Colloidal blue stained gel bands were destained in 50% acetonitrile/50mM Tris pH 8.1 until clear. The bands were then reduced with 40 mM TCEP/50mM Tris, pH 8.1 and alkylated with 20mM iodoacetamide/50mM Tris

pH 8.1 at room temperature for 90 mins in the dark. Proteins were digested in-situ with 50ul (0.005ug/ul) trypsin (Promega Corporation, Madison WI) in 20 mM Tris pH 8.1 / 0.0002% Zwittergent 3–16, at 37°C for 16 hours, followed by peptide extraction with 20ul of 2% trifluoroacetic acid and 80ul of acetonitrile. The pooled extracts are concentrated to less than 5ul on a SpeedVac spinning concentrator (Savant Instruments, Holbrook NY) and then brought up in 0.2% trifluoroacetic acid for protein identification by nano-flow liquid chromatography electrospray tandem mass spectrometry (nanoLC-ESI-MS/MS) using a ThermoFinnigan QExactive™ Mass Spectrometer (Thermo Fisher Scientific, Bremen, Germany) coupled to an Eksigent nanoLC-2D HPLC system (Eksigent, Dublin, CA). The digest peptide mixture is loaded onto a 250nl OPTI-PAK trap (Optimize Technologies, Oregon City, OR) custom packed with Michrom Magic C8 solid phase (Michrom Bioresources, Auburn, CA). Chromatography is performed using 0.2 % formic acid in both the A solvent (98% water/2% acetonitrile) and B solvent (80% acetonitrile/10% isopropanol/10% water), and a 2%B to 40%B gradient over 160 minutes at 300 nl/min through a hand packed PicoFrit (New Objective, Woburn, MA) 75μm × 300mm column (Agilent PoroShell EC-C18, 2.7um). The Q-Exactive™ MS method measured peptide molecular weights using 70,000 resolving power (FWHM, m/z 200) survey scans (MS1) followed by automated accurate mass MS/MS experiments of the top 20 abundant precursor masses (charge states 2–5, inclusive). MS/MS spectra were extracted from the raw data files using msconvert (proteowizard.sourceforge.net) to generate input search files for assigning peptide sequence to tandem mass spectra. MS2 spectra were searched against Uniprot (June 2013) using the MyriMatch search engine[51] Peptide spectral matches (PSM) were then qualified using IDPicker[52]. Proteins were matched at a FDR of < 1% with a 2 peptide match minimum.

## Characterization of Method Variability

The coefficient of variance (CV) of all identified peptides within the 7 control subjects, for each gel section, was calculated from the MS1 abundance of each identified peptide. The median CV was 0.48 (IQR = 0.33, $10^{th}$ percentile = 0.25, $90^{th}$ percentile = 0.93, n=45595) after Loess normalization within each gel section (median CV = 0.54, IQR = 0.31 without data normalization) and similar to results from the urinary proteome reported by Nagaraj *et al* who reported inter-subject variability of 0.66.[53]

Overall variability for the relative quantification of any peptide is a composite of variability in the analytical methodology, variability between individuals, and variability from intra-individual physiological differences such as the time of urine sample collection. We assessed contributions to this overall variability at 3 levels: 1) the synthetic peptide angiotensin-I was spiked into each sample prior to LC-MS to assess variability at the instrument level (LC-MS/MS). 2) independent of this study, we processed aliquots of yeast lysate in 7 gel lanes, and excised, digested, and performed LC-MS/MS analyses from a gel section comprising proteins from the 37–48 kDa range to assess for variability without using data normalization methods 3) Three protein internal standards were added to each sample at the 200 fmol level prior to gel analysis to be measured in parallel with the exosome proteome from each subject median CV of all peptides from the internal standards assessed with and without normalization. After Loess normalization, the median CV of the three

internal standards increased from 0.22 to 0.30 while the median cv of all peptides in the data set, comprised primarily of the biological replicates, was reduced from 0.54 to 0.48 post-normalization- further evidence that biological variability is greater than the technical variability of our analytical protocol and therefore instrument time is better spent analyzing additional biological replicates rather than analyzing technical replicates of biological samples.

### Bioinformatics

Acquired MS features from the LTQ-Orbitrap were analyzed with Rosetta Elucidator and automatically processed by our analysis pipeline. ID mapping was compared to Uniprot facilitating comparison of our proteome with urine, glomerular & existing exosome proteomes. All reference proteomes used in the comparison were compared using Uniprot IDs and DAVID database version 6.7.[54]. We obtained the initial list of proteins in Fractions B and C by intersecting results from Swift (Mascot version 2.2.04 (Matrix Science Ltd, London, England), Sequest version 27.12 (Thermo Fisher Scientific, San Jose, California), X!Tandem (version 2006.09.15.3; Global Proteome Machine Organization, http://www.thegpm.org), Scaffold (version 3 00 03) & combined data set from Elucidator.[55] The Scaffold result was filtered using 95% protein probability, 95% peptide probability, at least 2 spectra identified per protein. Protein export files into Excel were created using the filtering conditions highlighted above. For the inter-individual analysis the list of 1500 common proteins identified by both Swift and Elucidator pipelines was reduced from 1700 proteins (at detectable levels) to 1500 proteins (at quantifiable level). Additionally, trypsin, the spike-in protein internal standards, and any reversed sequence protein hits (decoy hits) were removed from the export list that was used for the Venn diagrams and generated with VENNY.[56]

## Supplementary Material

Refer to Web version on PubMed Central for supplementary material.

## Acknowledgements

The authors (MCH and CJW) acknowledge support from NIH Grants 1RC1DK086161-01 (MPI) GRANT10266762 and NIDDK P30 DK090728 to and a Pilot Study award from the NephCure Foundation to MCH as supported in the NEPTUNE study (from the NIH Office of Rare Diseases (U-54DK083912), the patients and volunteers. The Proteomics Core is supported by Mr. and Mrs. Gordon C. Gilroy, the David Woods Kemper Memorial Foundation and the Mayo Clinic College of Medicine. We thank Drs. Kershaw and Wiggins (U Michigan) for the gift of podocalyxin antibody, Drs. Peter Harris and Samih Nasr for helpful comments on the manuscript. A portion of this work was presented in abstract form at the 2010 Annual Meeting of the American Society of Nephrology Denver, Colorado, November 16–21, 2010.

## References

1. Keller S, Sanderson MP, Stoeck A, et al. Exosomes: from biogenesis and secretion to biological function. Immunology Letters. 2006; 107:102–108. [PubMed: 17067686]
2. Johnstone RM, Adam M, Hammond JR, et al. Vesicle formation during reticulocyte maturation. Association of plasma membrane activities with released vesicles (exosomes). Journal of Biological Chemistry. 1987; 262:9412–9420. [PubMed: 3597417]
3. Johnstone RM. Revisiting the road to the discovery of exosomes. Blood Cells Molecules & Diseases. 2005; 34:214–219.

4. Pisitkun T, Shen RF, Knepper MA. Identification and proteomic profiling of exosomes in human urine. Proc Natl Acad Sci U S A. 2004; 101:13368–13373. [PubMed: 15326289]
5. Pisitkun T, Johnstone R, Knepper MA. Discovery of urinary biomarkers. Molecular & Cellular Proteomics. 2006; 5:1760–1771. [PubMed: 16837576]
6. Knepper MA, Pisitkun T. Exosomes in urine: who would have thought…? Kidney Int. 2007; 72:1043–1045. [PubMed: 17943150]
7. Bayer ME. An Electron Microscope Examination of Urinary Mucoprotein and Its Interaction with Influenza Virus. J Cell Biol. 1964; 21:265–274. [PubMed: 14159029]
8. Fernandez-Llama P, Khositseth S, Gonzales PA, et al. Tamm-Horsfall protein and urinary exosome isolation. Kidney Int. 77:736–742. [PubMed: 20130532]
9. Hiemstra TF, Charles PD, Hester SS, et al. Uromodulin exclusion list improves urinary exosomal protein identification. J Biomol Tech. 2011; 22:136–145. [PubMed: 22131889]
10. Hogan MC, Manganelli L, Woollard JR, et al. Characterization of PKD Protein-Positive Exosome-Like Vesicles. J Am Soc Nephrol. 2009; 20:278–288. [PubMed: 19158352]
11. Arac D, Boucard AA, Bolliger MF, et al. A novel evolutionarily conserved domain of cell-adhesion GPCRs mediates autoproteolysis. Embo J. 2012; 31:1364–1378. [PubMed: 22333914]
12. Bakeberg JL, Tammachote R, Woollard JR, et al. Epitope-tagged Pkhd1 tracks the processing, secretion, and localization of fibrocystin. J Am Soc Nephrol. 2011; 22:2266–2277. [PubMed: 22021705]
13. Gonzales PA, Pisitkun T, Hoffert JD, et al. Large-scale proteomics and phosphoproteomics of urinary exosomes. J Am Soc Nephrol. 2009; 20:363–379. [PubMed: 19056867]
14. Zhou H, Yuen PS, Pisitkun T, et al. Collection, storage, preservation, and normalization of human urinary exosomes for biomarker discovery. Kidney International. 2006; 69:1471–1476. [PubMed: 16501490]
15. Wang Z, Hill S, Luther JM, et al. Proteomic analysis of urine exosomes by multidimensional protein identification technology (MudPIT). Proteomics. 2012; 12:329–338. [PubMed: 22106071]
16. Raj DAA, Fiume I, Capasso G, et al. A multiplex quantitative proteomics strategy for protein biomarker studies in urinary exosomes. Kidney Int. 2012
17. Kershaw DB, Beck SG, Wharram BL, et al. Molecular cloning and characterization of human podocalyxin-like protein. Orthologous relationship to rabbit PCLP1 and rat podocalyxin. J Biol Chem. 1997; 272:15708–15714. [PubMed: 9188463]
18. Mundel P, Shankland SJ. Podocyte biology and response to injury. J Am Soc Nephrol. 2002; 13:3005–3015. [PubMed: 12444221]
19. Miyamoto M, Yoshida Y, Taguchi I, et al. In-Depth Proteomic Profiling of the Normal Human Kidney Glomerulus Using Two-Dimensional Protein Prefractionation in Combination with Liquid Chromatography-Tandem Mass Spectrometry. Journal of proteome research. 2007; 6:3680–3690. [PubMed: 17711322]
20. Hogan, M. JASN. Denver, CO: 2010 Nov. In-Depth Proteomic Analysis of Podocin-Rich Exosomes in Human Urine; p. F-PO1996
21. Neubert H, Bonnert TP, Rumpel K, et al. Label-free detection of differential protein expression by LC/MALDI mass spectrometry. Journal of proteome research. 2008; 7:2270–2279. [PubMed: 18412385]
22. Wiener MC, Sachs JR, Deyanova EG, et al. Differential mass spectrometry: a label-free LC-MS method for finding significant differences in complex peptide and protein mixtures. Anal Chem. 2004; 76:6085–6096. [PubMed: 15481957]
23. New Aspects of Membranoproliferative Glomerulonephritis. New England Journal of Medicine. 2012; 367:86–87. [PubMed: 22762333]
24. Vitureira N, Andrés R, Pérez-Martínez E, et al. Podocalyxin Is a Novel Polysialylated Neural Adhesion Protein with Multiple Roles in Neural Development and Synapse Formation. PloS one. 2010; 5:e12003. [PubMed: 20706633]
25. Douglas Lu W, Funkelstein L, Toneff T, et al. Cathepsin H functions as an aminopeptidase in secretory vesicles for production of enkephalin and galanin peptide neurotransmitters. J Neurochem. 2012

26. Hu N, Westra J, Kallenberg CG. Membrane-bound proteinase 3 and its receptors: relevance for the pathogenesis of Wegener's Granulomatosis. Autoimmun Rev. 2009; 8:510–514. [PubMed: 19185066]
27. Michalski A, Damoc E, Hauschild JP, et al. Mass spectrometry-based proteomics using Q Exactive, a high-performance benchtop quadrupole Orbitrap mass spectrometer. Molecular & cellular proteomics : MCP. 2011; 10:M111 011015. [PubMed: 21642640]
28. Hara M, Yanagihara T, Kihara I, et al. Apical cell membranes are shed into urine from injured podocytes: a novel phenomenon of podocyte injury. J Am Soc Nephrol. 2005; 16:408–416. [PubMed: 15625073]
29. Hara M, Yanagihara T, Hirayama Y, et al. Podocyte membrane vesicles in urine originate from tip vesiculation of podocyte microvilli. Human Pathology. 2010 Sep; 41(9):1265–1275. Epub 2010 May 5.; **41** 1265–1275. [PubMed: 20447677]
30. Fernandez D, Larrucea S, Nowakowski A, et al. Release of podocalyxin into the extracellular space Role of metalloproteinases. Biochim Biophys Acta. 2011; 1813:1504–1510. [PubMed: 21616097]
31. Musante L, Saraswat M, Duriez E, et al. Biochemical and physical characterisation of urinary nanovesicles following CHAPS treatment. PloS one. 2012; 7:e37279. [PubMed: 22808001]
32. Ruotsalainen V, Ljungberg P, Wartiovaara J, et al. Nephrin is specifically located at the slit diaphragm of glomerular podocytes. Proceedings of the National Academy of Sciences. 1999; 96:7962–7967.
33. Winn MP, Conlon PJ, Lynn KL, et al. A Mutation in the TRPC6 Cation Channel Causes Familial Focal Segmental Glomerulosclerosis. Science. 2005
34. Reiser J, Polu KR, Moller CC, et al. TRPC6 is a glomerular slit diaphragm-associated channel required for normal renal function. Nat Genet. 2005; 37:739–744. [PubMed: 15924139]
35. Beck LH, Bonegio RGB, Lambeau G, et al. M-Type Phospholipase A(sub 2) Receptor as Target Antigen in Idiopathic Membranous Nephropathy. New England Journal of Medicine. 2009; 361:11–21. [PubMed: 19571279]
36. Zhou H, Cheruvanky A, Hu X, et al. Urinary exosomal transcription factors, a new class of biomarkers for renal disease. Kidney Int. 2008; 74:613–621. [PubMed: 18509321]
37. Hill GS, Karoui KE, Karras A, et al. Focal segmental glomerulosclerosis plays a major role in the progression of IgA nephropathy. I. Immunohistochemical studies. Kidney Int. 2011; 79:635–642. [PubMed: 21160460]
38. Dewald B, Rindlerludwig R, Bretz U, et al. Subcellular-Localization and Heterogeneity of Neutral Proteases in Neutrophilic Polymorphonuclear Leukocytes. Journal of Experimental Medicine. 1975; 141:709–723. [PubMed: 236354]
39. Csernok E, Ludemann J, Gross WL, et al. Ultrastructural localization of proteinase 3, the target antigen of anti-cytoplasmic antibodies circulating in Wegener's granulomatosis. The American journal of pathology. 1990; 137:1113–1120. [PubMed: 2240162]
40. Gupta S, Niles J, McCluskey R, et al. Identity of Wegener's autoantigen (p29) with proteinase 3 and myeloblastin [letter]. Blood. 1990; 76:2162. [PubMed: 2242436]
41. Gabay JE, Scott RW, Campanelli D, et al. Antibiotic proteins of human polymorphonuclear leukocytes. Proceedings of the National Academy of Sciences. 1989; 86:5610–5614.
42. Campanelli D, Melchior M, Fu Y, et al. Cloning of cDNA for proteinase 3: a serine protease, antibiotic, and autoantigen from human neutrophils. The Journal of Experimental Medicine. 1990; 172:1709–1715. [PubMed: 2258701]
43. Gonzales PA, Pisitkun T, Hoffert JD, et al. Large-scale proteomics and phosphoproteomics of urinary exosomes. Journal of the American Society of Nephrology : JASN. 2009; 20:363–379. [PubMed: 19056867]
44. Rood IM, Deegens JKJ, Merchant ML, et al. Comparison of three methods for isolation of urinary microvesicles to identify biomarkers of nephrotic syndrome. Kidney Int.
45. Cheruvanky A, Zhou H, Pisitkun T, et al. Rapid isolation of urinary exosomal biomarkers using a nanomembrane ultrafiltration concentrator. American Journal of Physiology - Renal Physiology. 2007; 292:F1657–F1661. [PubMed: 17229675]

46. Keller A, Nesvizhskii AI, Kolker E, et al. Empirical statistical model to estimate the accuracy of peptide identifications made by MS/MS and database search. Anal Chem. 2002; 74:5383–5392. [PubMed: 12403597]
47. Bradshaw RA, Burlingame AL, Carr S, et al. Reporting Protein Identification Data: The next Generation of Guidelines. Molecular & Cellular Proteomics. 2006; 5:787–788. [PubMed: 16670253]
48. Käll L, Storey JD, MacCoss MJ, et al. Assigning Significance to Peptides Identified by Tandem Mass Spectrometry Using Decoy Databases. Journal of proteome research. 2007; 7:29–34. [PubMed: 18067246]
49. Nesvizhskii AI, Keller A, Kolker E, et al. A Statistical Model for Identifying Proteins by Tandem Mass Spectrometry. Anal Chem. 2003; 75:4646–4658. [PubMed: 14632076]
50. Elias JE, Gygi SP. Target-decoy search strategy for increased confidence in large-scale protein identifications by mass spectrometry. Nat Methods. 2007; 4:207–214. [PubMed: 17327847]
51. Tabb DL, Fernando CG, Chambers MC. MyriMatch: Highly Accurate Tandem Mass Spectral Peptide Identification by Multivariate Hypergeometric Analysis. Journal of proteome research. 2007; 6:654–661. [PubMed: 17269722]
52. Ma Z-Q, Dasari S, Chambers MC, et al. IDPicker 2.0: Improved Protein Assembly with High Discrimination Peptide Identification Filtering. Journal of proteome research. 2009; 8:3872–3881. [PubMed: 19522537]
53. Nagaraj N, Mann M. Quantitative analysis of the intra- and inter-individual variability of the normal urinary proteome. Journal of proteome research. 2011; 10:637–645. [PubMed: 21126025]
54. Huang DW, Sherman BT, Lempicki RA. Systematic and integrative analysis of large gene lists using DAVID bioinformatics resources. Nat Protocols. 2008; 4:44–57.
55. Searle BC, Turner M, Nesvizhskii AI. Improving Sensitivity by Probabilistically Combining Results from Multiple MS/MS Search Methodologies. Journal of proteome research. 2008; 7:245–253. [PubMed: 18173222]
56. Oliveros J. VENNY. An interactive tool for comparing lists with Venn Diagrams. 2007
57. Assmann KJ, Koene RA, Wetzels JF. Familial glomerulonephritis characterized by massive deposits of fibronectin. American journal of kidney diseases : the official journal of the National Kidney Foundation. 1995; 25:781–791. [PubMed: 7747733]
58. Strom EH, Banfi G, Krapf R, et al. Glomerulopathy associated with predominant fibronectin deposits: a newly recognized hereditary disease. Kidney International. 1995; 48:163–170. [PubMed: 7564073]
59. Kantarci S, Al-Gazali L, Hill RS, et al. Mutations in LRP2, which encodes the multiligand receptor megalin, cause Donnai-Barrow and facio-oculo-acousticorenal syndromes. Nat Genet. 2007; 39:957–959. [PubMed: 17632512]
60. Kerjaschki D, Farquhar MG. Immunocytochemical localization of the Heymann nephritis antigen (GP330) in glomerular epithelial cells of normal Lewis rats. Journal of Experimental Medicine. 1983; 157:667–686. [PubMed: 6337231]
61. Storm T, Emma F, Verroust PJ, et al. A patient with cubilin deficiency. The New England journal of medicine. 2011; 364:89–91. [PubMed: 21208123]
62. Ovunc B, Ashraf S, Vega-Warner V, et al. Mutation analysis of NPHS1 in a worldwide cohort of congenital nephrotic syndrome patients. Nephron Clinical practice. 2012; 120:c139–c146. [PubMed: 22584503]
63. Fremeaux-Bacchi V, Miller EC, Liszewski MK, et al. Mutations in complement C3 predispose to development of atypical hemolytic uremic syndrome. Blood. 2008; 112:4948–4952. [PubMed: 18796626]
64. Geerdink L, Westra D, van Wijk J, et al. Atypical hemolytic uremic syndrome in children: complement mutations and clinical characteristics. Pediatric Nephrology. 2012; 27:1283–1291. [PubMed: 22410797]
65. Fremeaux-Bacchi V, Dragon-Durey MA, Blouin J, et al. Complement factor I: a susceptibility gene for atypical haemolytic uraemic syndrome. J Med Genet. 2004; 41:e84. [PubMed: 15173250]
66. Heath KE, Campos-Barros A, Toren A, et al. Nonmuscle myosin heavy chain IIA mutations define a spectrum of autosomal dominant macrothrombocytopenias: May-Hegglin anomaly and Fechtner,

Sebastian, Epstein, and Alport-like syndromes. Am J Hum Genet. 2001; 69:1033–1045. [PubMed: 11590545]

67. Johnstone DB, Zhang J, George B, et al. Podocyte-Specific Deletion of Myh9 Encoding Nonmuscle Myosin Heavy Chain 2A Predisposes Mice to Glomerulopathy. Molecular and Cellular Biology. 2011; 31:2162–2170. [PubMed: 21402784]
68. Ozaltin F, Ibsirlioglu T, Taskiran Ekim Z, et al. Disruption of PTPRO Causes Childhood-Onset Nephrotic Syndrome. The American Journal of Human Genetics. **In Press, Corrected Proof**.
69. Ozaltin F, Ibsirlioglu T, Taskiran Ekim Z, et al. Disruption of PTPRO Causes Childhood-Onset Nephrotic Syndrome. The American Journal of Human Genetics. 2011; 89:139–147. [PubMed: 21722858]
70. Tawadrous H, Maga T, Sharma J, et al. A novel mutation in the Complement Factor B gene (<i>CFB</i>) and atypical hemolytic uremic syndrome. Pediatric Nephrology. 2010; 25:947–951. [PubMed: 20108004]
71. Shih NY, Li J, Karpitskii V, et al. Congenital nephrotic syndrome in mice lacking CD2-associated protein. Science. 1999; 286:312–315. [PubMed: 10514378]
72. Kim JM, Wu H, Green G, et al. CD2-Associated Protein Haploinsufficiency Is Linked to Glomerular Disease Susceptibility. Science. 2003; 300:1298–1300. [PubMed: 12764198]
73. Abe K, Miyazaki M, Koji T, et al. Expression of decay accelerating factor mRNA and complement C3 mRNA in human diseased kidney. Kidney Int. 1998; 54:120–130. [PubMed: 9648070]
74. Shibata T, Cosio FG, Birmingham DJ. Complement activation induces the expression of decay-accelerating factor on human mesangial cells. J Immunol. 1991; 147:3901–3908. [PubMed: 1719094]
75. Ben-Smith A, Dove SK, Martin A, et al. Antineutrophil cytoplasm autoantibodies from patients with systemic vasculitis activate neutrophils through distinct signaling cascades: comparison with conventional Fcγ receptor ligation. Blood. 2001; 98:1448–1455. [PubMed: 11520794]
76. Relle M, Cash H, Brochhausen C, et al. New perspectives on the renal slit diaphragm protein podocin. Mod Pathol. 2011; 24:1101–1110. [PubMed: 21499232]
77. Lowenthal, Ja, editor. Kidney Biopsy Interpretation. Introduction.
78. Karamatic Crew V, Burton N, Kagan A, et al. CD151, the first member of the tetraspanin (TM4) superfamily detected on erythrocytes, is essential for the correct assembly of human basement membranes in kidney and skin. Blood. 2004; 104:2217–2223. [PubMed: 15265795]
79. Sachs N, Kreft M, van den Bergh Weerman MA, et al. Kidney failure in mice lacking the tetraspanin CD151. J Cell Biol. 2006; 175:33–39. [PubMed: 17015618]
80. Yoo SH, Lee K, Chae JY, et al. CD151 expression can predict cancer progression in clear cell renal cell carcinoma. Histopathology. 2011; 58:191–197. [PubMed: 21323946]
81. Roselli S, Baleato RM, Guthrie PL, et al. Deletion of Cd151 results in a strain-dependent glomerular disease due to severe alterations of the glomerular basement membrane. American Journal of Pathology. 2008; 173:927–937. [PubMed: 18787104]
82. Sachs N, Claessen N, Aten J, et al. Blood pressure influences end-stage renal disease of Cd151 knockout mice. The Journal of Clinical Investigation. 2012; 122:348–358. [PubMed: 22201679]
83. Has C, Spartà G, Kiritsi D, et al. Integrin α3 Mutations with Kidney, Lung, and Skin Disease. New England Journal of Medicine. 2012; 366:1508–1514. [PubMed: 22512483]
84. Nicolaou N, Margadant C, Kevelam SH, et al. Gain of glycosylation in integrin α3 causes lung disease and nephrotic syndrome. The Journal of Clinical Investigation. 2012; 0
85. Gupta IR, Baldwin C, Auguste D, et al. ARHGDIA: a novel gene implicated in nephrotic syndrome. Journal of Medical Genetics. 2013; 50:330–338. [PubMed: 23434736]
86. Gee HY, Saisawat P, Ashraf S, et al. ARHGDIA mutations cause nephrotic syndrome via defective RHO GTPase signaling. The Journal of Clinical Investigation. 2013; 123:0–0.
87. Groffen AJA, Buskens CAF, van Kuppevelt TH, et al. Primary structure and high expression of human agrin in basement membranes of adult lung and kidney. European Journal of Biochemistry. 1998; 254:123–128. [PubMed: 9652404]

88. Mele C, Iatropoulos P, Donadelli R, et al. MYO1E Mutations and Childhood Familial Focal Segmental Glomerulosclerosis. New England Journal of Medicine. 2011; 365:295–306. [PubMed: 21756023]

89. Kuźniar J, Kuźniar TJ, Marchewka Z, et al. Elastase deposits in the kidney and urinary elastase excretion in patients with glomerulonephritis - evidence for neutrophil involvement in renal injury. Scandinavian Journal of Urology & Nephrology. 2007; 41:527–534. [PubMed: 17853021]

90. Boyer O, Nevo F, Plaisier E, et al. INF2 Mutations in Charcot–Marie–Tooth Disease with Glomerulopathy. New England Journal of Medicine. 2011; 365:2377–2388. [PubMed: 22187985]

91. Roesli C, Fugmann T, Borgia B, et al. Proteomic identification of vanin-1 as a marker of kidney damage in a rat model of type 1 diabetic nephropathy. Kidney International. 2011; 80:272–281. [PubMed: 21544065]

92. Krendel M, Kim SV, Willinger T, et al. Disruption of Myosin 1e promotes podocyte injury. J Am Soc Nephrol. 2009; 20:86–94. [PubMed: 19005011]

93. Sanna-Cherchi S, Burgess KE, Nees SN, et al. Exome sequencing identified MYO1E and NEIL1 as candidate genes for human autosomal recessive steroid-resistant nephrotic syndrome. Kidney Int. 2011; 80:389–396. [PubMed: 21697813]

94. Kain R, Exner M, Brandes R, et al. Molecular mimicry in pauci-immune focal necrotizing glomerulonephritis. Nat Med. 2008; 14:1088–1096. [PubMed: 18836458]

95. Kawakami T, Takeuchi S, Arimura Y, et al. Elevated antilysosomal-associated membrane protein-2 antibody levels in patients with adult Henoch-Schonlein purpura. The British journal of dermatology. 2012; 166:1206–1212. [PubMed: 22309950]

96. Kobayashi T, Notoya M, Shinosaki T, et al. Cortactin interacts with podocalyxin and mediates morphological change of podocytes through its phosphorylation. Nephron Exp Nephrol. 2009; 113:e89–e96. [PubMed: 19684413]

97. Huang T-H, Shui H-A, Ka S-M, et al. Rab 23 is expressed in the glomerulus and plays a role in the development of focal segmental glomerulosclerosis. Nephrology Dialysis Transplantation. 2009; 24:743–754.

98. Fugmann T, Borgia B, Revesz C, et al. Proteomic identification of vanin-1 as a marker of kidney damage in a rat model of type 1 diabetic nephropathy. Kidney Int. 2011; 80:272–281. [PubMed: 21544065]

99. Hugo C, Nangaku M, Shankland SJ, et al. The plasma membrane-actin linking protein, ezrin, is a glomerular epithelial cell marker in glomerulogenesis, in the adult kidney and in glomerular injury. Kidney International. 1998; 54:1934–1944. [PubMed: 9853258]

100. Saburi S, Hester I, Fischer E, et al. Loss of Fat4 disrupts PCP signaling and oriented cell division and leads to cystic kidney disease. Nat Genet. 2008; 40:1010–1015. [PubMed: 18604206]

101. Turnberg D, Botto M, Warren J, et al. CD59a Deficiency Exacerbates Accelerated Nephrotoxic Nephritis in Mice. Journal of the American Society of Nephrology. 2003; 14:2271–2279. [PubMed: 12937303]

102. Praekelt U, Kopp PM, Rehm K, et al. New isoform-specific monoclonal antibodies reveal different sub-cellular localisations for talin1 and talin2. European Journal of Cell Biology. 2012; 91:180–191. [PubMed: 22306379]

103. Fialka I, Steinlein P, Ahorn H, et al. Identification of Syntenin as a Protein of the Apical Early Endocytic Compartment in Madin-Darby Canine Kidney Cells. Journal of Biological Chemistry. 1999; 274:26233–26239. [PubMed: 10473577]

104. Westwood BM, Chappell MC. Divergent pathways for the angiotensin-(1–12) metabolism in the rat circulation and kidney. Peptides. 2012; 35:190–195. [PubMed: 22490446]

105. Debiec H, Guigonis V, Mougenot B, et al. Brief report - Antenatal membranous glomerulonephritis due to anti-neutral endopeptidase antibodies. New England Journal of Medicine. 2002; 346:2053–2060. [PubMed: 12087141]

106. Takeda T. Podocyte cytoskeleton is connected to the integral membrane protein podocalyxin through Na+/H+-exchanger regulatory factor 2 and ezrin. Clinical and Experimental Nephrology. 2003; 7:260–269. [PubMed: 14712354]

107. Tipnis SR, Hooper NM, Hyde R, et al. A Human Homolog of Angiotensin-converting Enzyme: CLONING AND FUNCTIONAL EXPRESSION AS A CAPTOPRIL-INSENSITIVE

CARBOXYPEPTIDASE. Journal of Biological Chemistry. 2000; 275:33238–33243. [PubMed: 10924499]

108. Ye M, Wysocki J, William J, et al. Glomerular Localization and Expression of Angiotensin-Converting Enzyme 2 and Angiotensin-Converting Enzyme: Implications for Albuminuria in Diabetes. Journal of the American Society of Nephrology. 2006; 17:3067–3075. [PubMed: 17021266]
109. Oberg AL, Vitek O. Statistical Design of Quantitative Mass Spectrometry-Based Proteomic Experiments. Journal of proteome research. 2009; 8:2144–2156. [PubMed: 19222236]

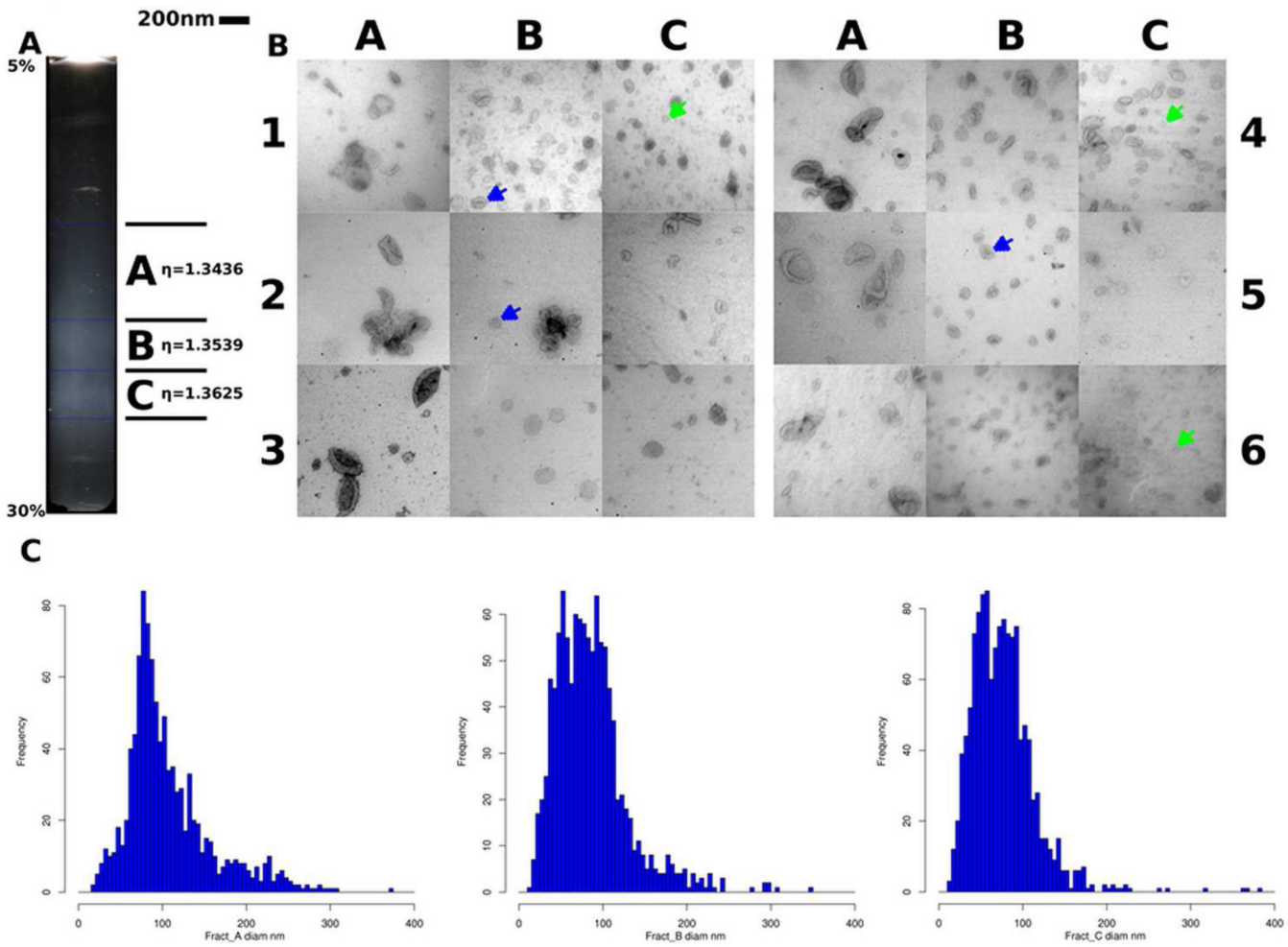


**Figure 1.**

Using density centrifugation of urine ELV pellets, three distinct subfractions are seen with the podocin-rich fraction corresponding to Zone C. **1A**. A transilluminated 5–30% sucrose heavy water gradient (following centrifugation of layered total ELV fraction). The white bands represent distinct ELV subpopulations. Fraction A is a low density diffuse band at the top, the B (PKD-ELV) fraction is of intermediate density and the C or glomerular membrane vesicle (GMV) fraction is of high density. **1B**. Transmission electron micrographs fractions A, B and C from six different normal individuals, viewed at 80,000×, [scale bar= 200nm]. Band A contains the largest diameter ELVs (150–300nm) with a biconcave 'punched out soccer ball' appearance, Band B (PKD-ELVs) contain classical ~100nm ELVs, (blue arrows). B and C contain classical ELVs and smaller amorphous GMVs (green arrows). **1C**. Size distribution of ELVs in fraction A, B and C, (we excluded any structures > 400nm, n=3406 ELVs, (measured from 6 individuals). Fraction A has a population of ELVs > 150nm and maximum diameter 310nm. The bulk of ELVs in fraction B are ~100nm with a small contribution from particles that are on average ~50nm in diameter, both contributing to the broad peak. Fraction C is bimodal with a large contribution from ~50nm glomerular membrane vesicles (GMVs).

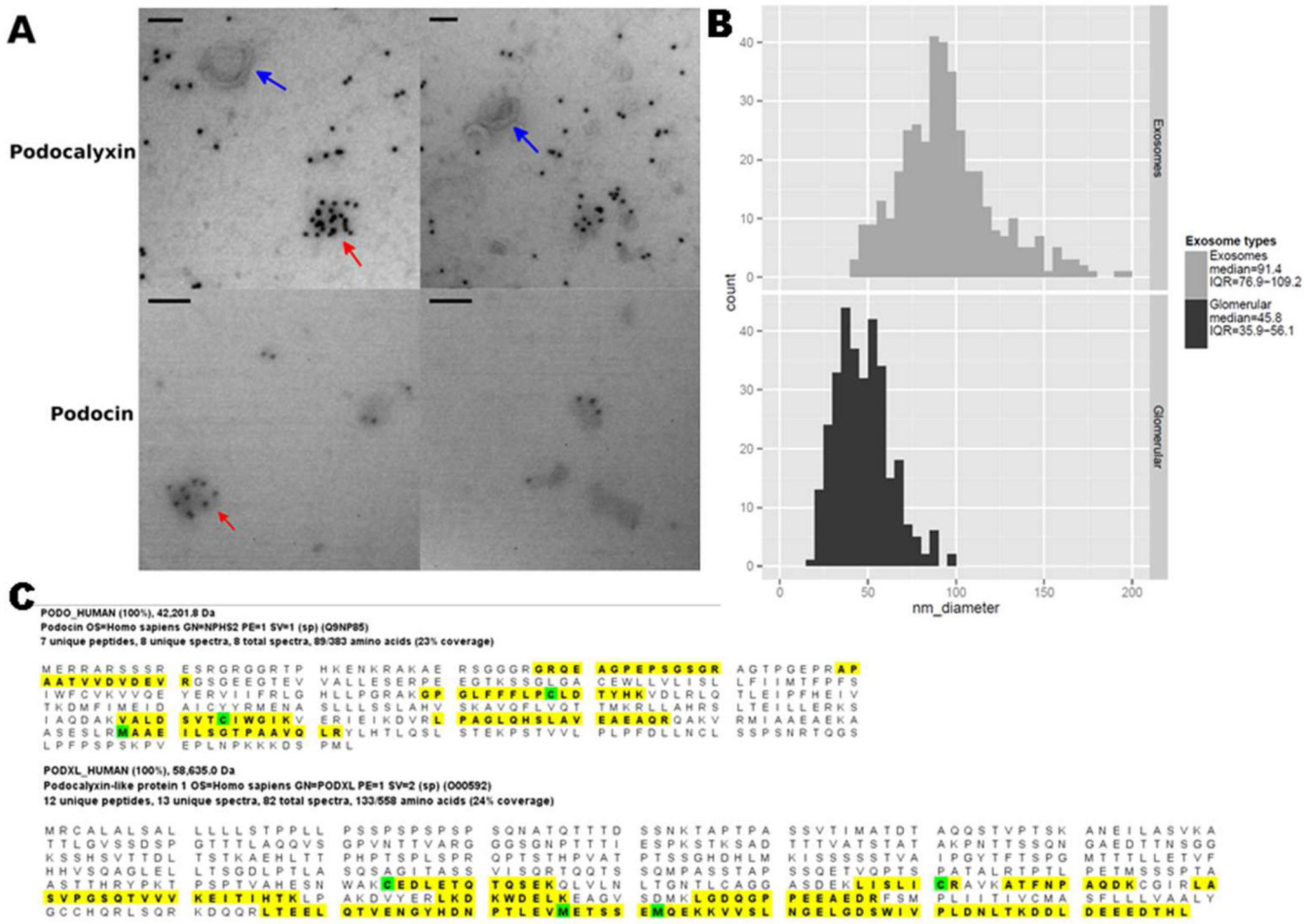


**Figure 2.**

Representative images of immuno-electron microscopy studies of GMVs: **2A**, shows GMVs stained with podocalyxin and podocin (red arrows) and classical podocalyxin /podocin negative ELVs (blue arrows) [Magnification: 80,000×, bars = 100nm]. **2B**, Size distribution of classical podocalyxin/podocin negative exosomes median 91.4 nm (IQR=76.9–109.2) and podocalyxin/podocin positive GMVs, median 45.8nm (IQR=35.9–56.1nm $p<2e^{-16}$; Wilcoxon). **2C**, Peptides identified for podocin (7 unique peptides; all 7 controls) and podocalyxin (57 unique peptides; all 7 controls) and were detected in each control and in the GelC (pooled urine) experiment.

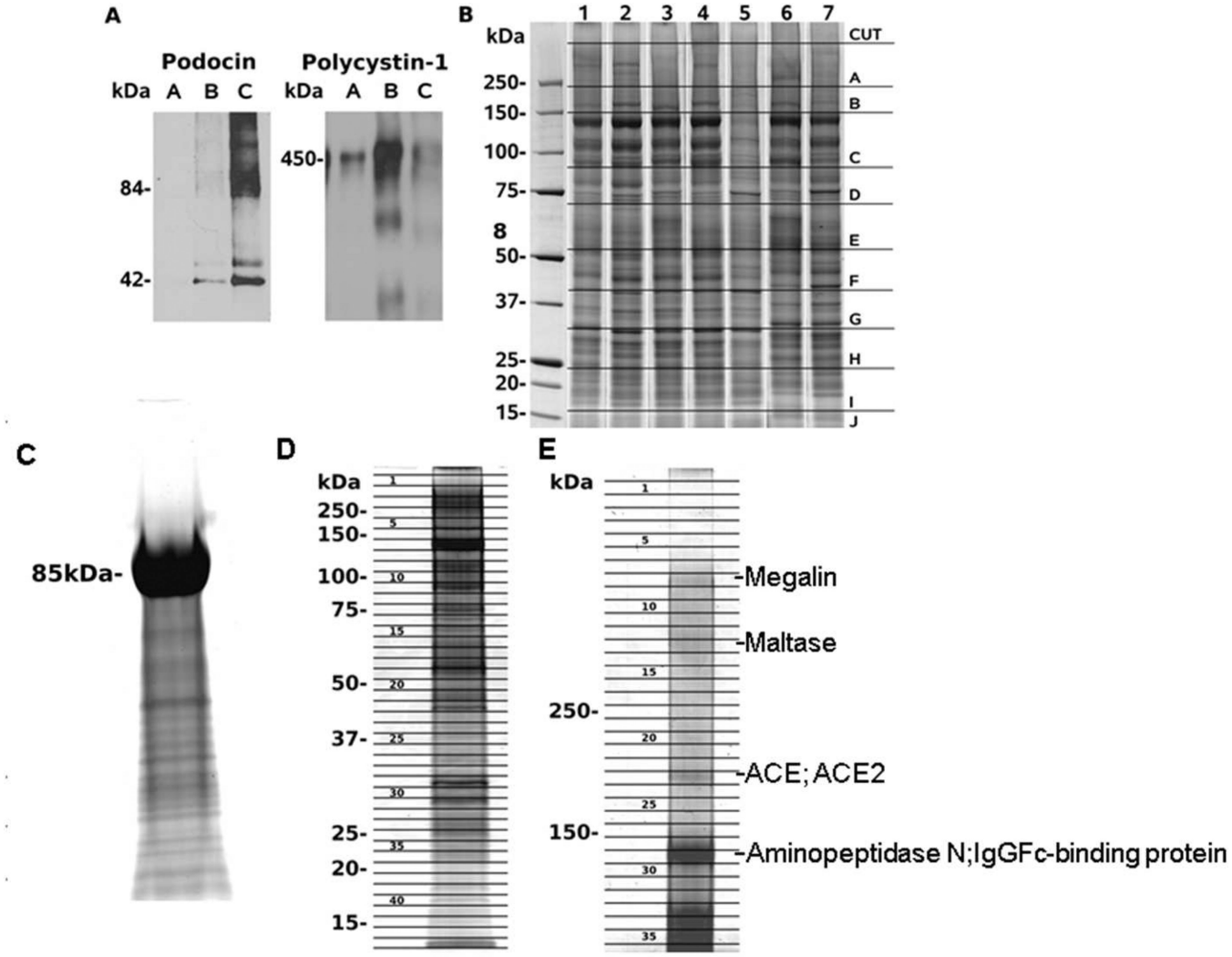

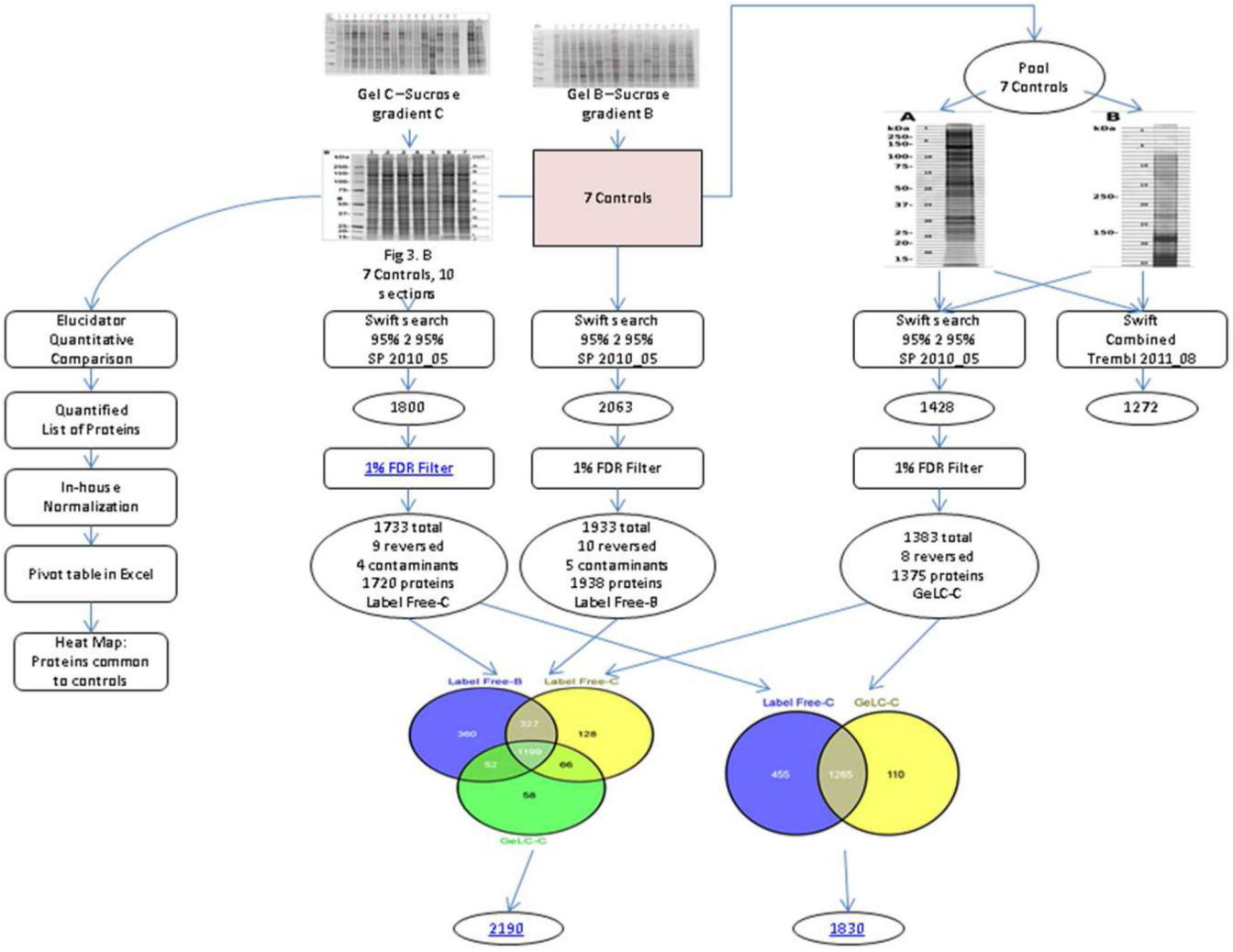


**Figure 3.**

**3A** Western blotting of 30μg of protein from fractions A, B and C probed with podocin (42kDa and 84kDa dimer) and polycystin-1 (7e12, IgG1k) (450kDa) antibodies. Podocin predominates in fraction C, whereas polycystin-1 predominates in fraction B. **3B**: Comparative inter-individual analysis on SDS PAGE (4–12%) of 30μg of fraction C protein, from 7 normal volunteers, cut into 10 slices per individual labeled A–J confirming analytical reproducibility of this method. These sections were used for proteomic analysis. **3C** reveals crude exosome product with abundant THP band at ~85kDa prior to density centrifugation. (GelC) analysis of human fraction C ELVs, showing gel slices corresponding to molecular weight data. **3D** Shows the low molecular weight slices (45 slices) and **3E** shows the sections sliced for the high molecular weight analysis of pooled samples (36 slices). Proteins of interest identified as most abundant corresponding to specific gel slices are marked. **3F** Summary of methodologies and post MS/MS data processing for protein identification and quantification.

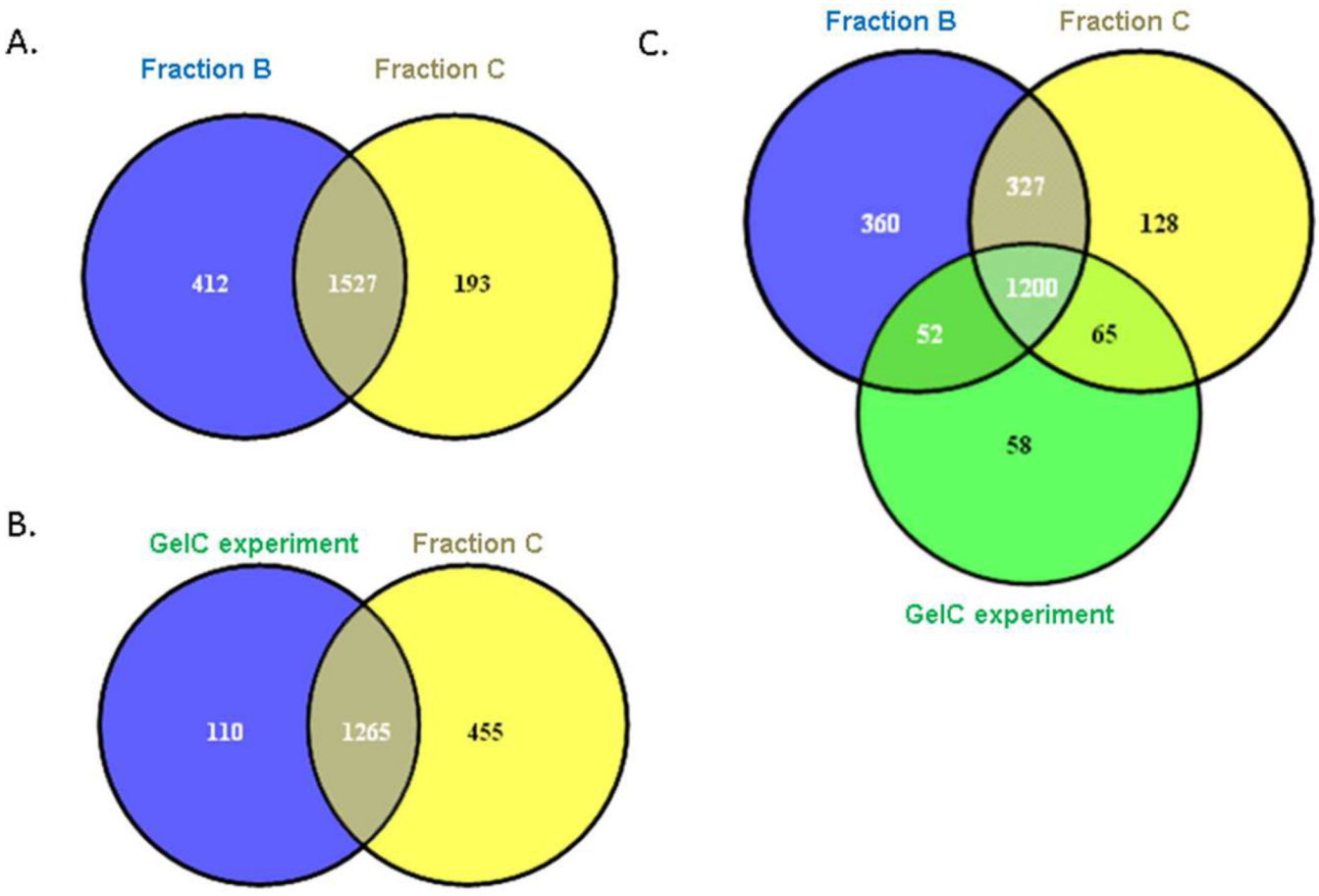


**Figure 4.**

Venn diagrams show overlap of various proteomic data: **4A**. Overlap of Fraction B and Fraction C proteomes. **4B**: Overlap of Gel C (pooled samples) and Fraction C proteomes i.e. total GMV proteome. **4C**: 2190 unique proteins were identified in all three experiments.

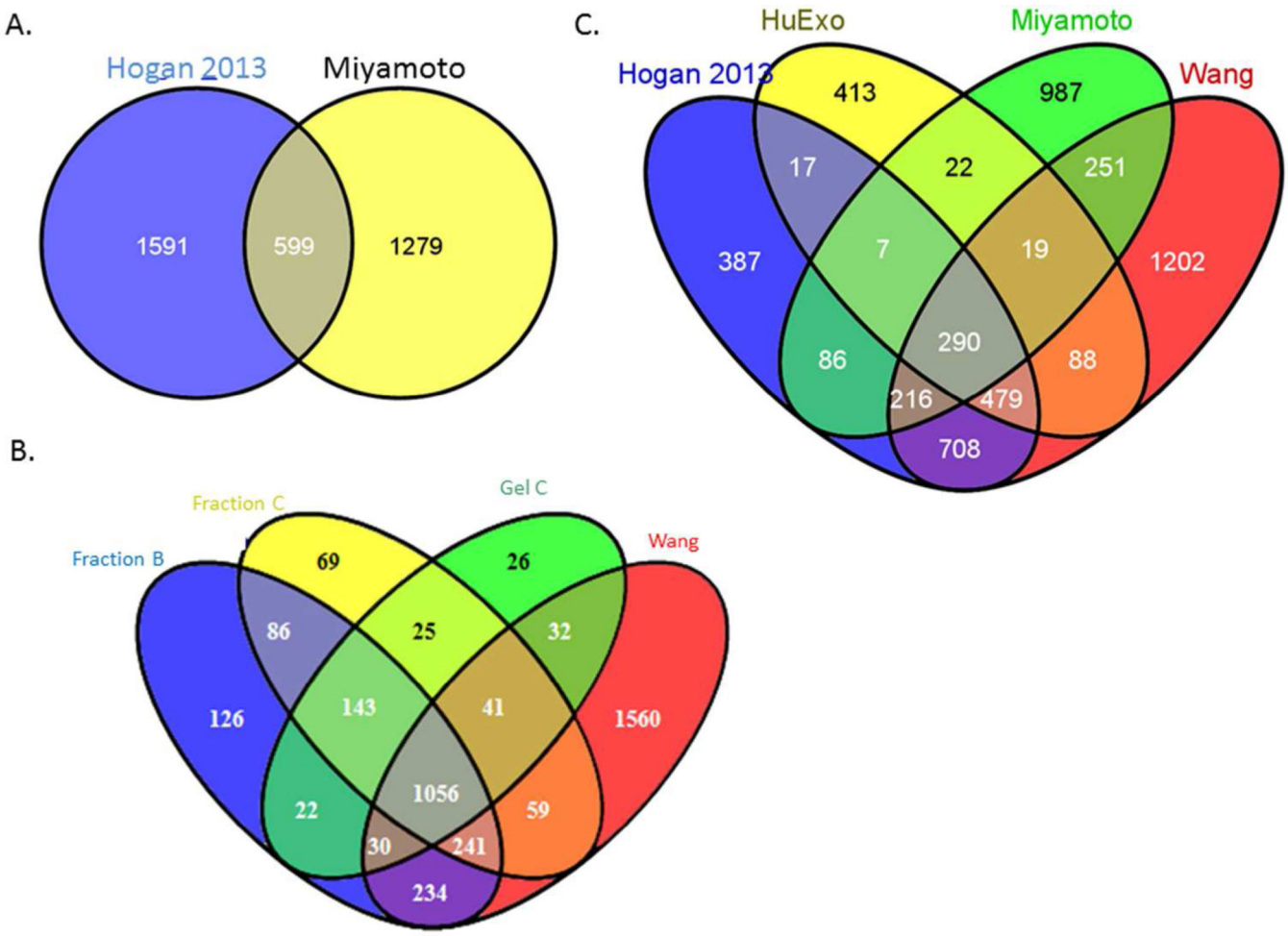


**Figure 5.**

**5A**. Venny diagram comparison of our proteome with the Miyamoto glomerular tissue proteome. **5B** Overlap of our data with the Wang *et al*. exosome proteome. **5C**. Comparison of human urine (NHLBI), Miyamoto and Wang exosome proteomes with our data.

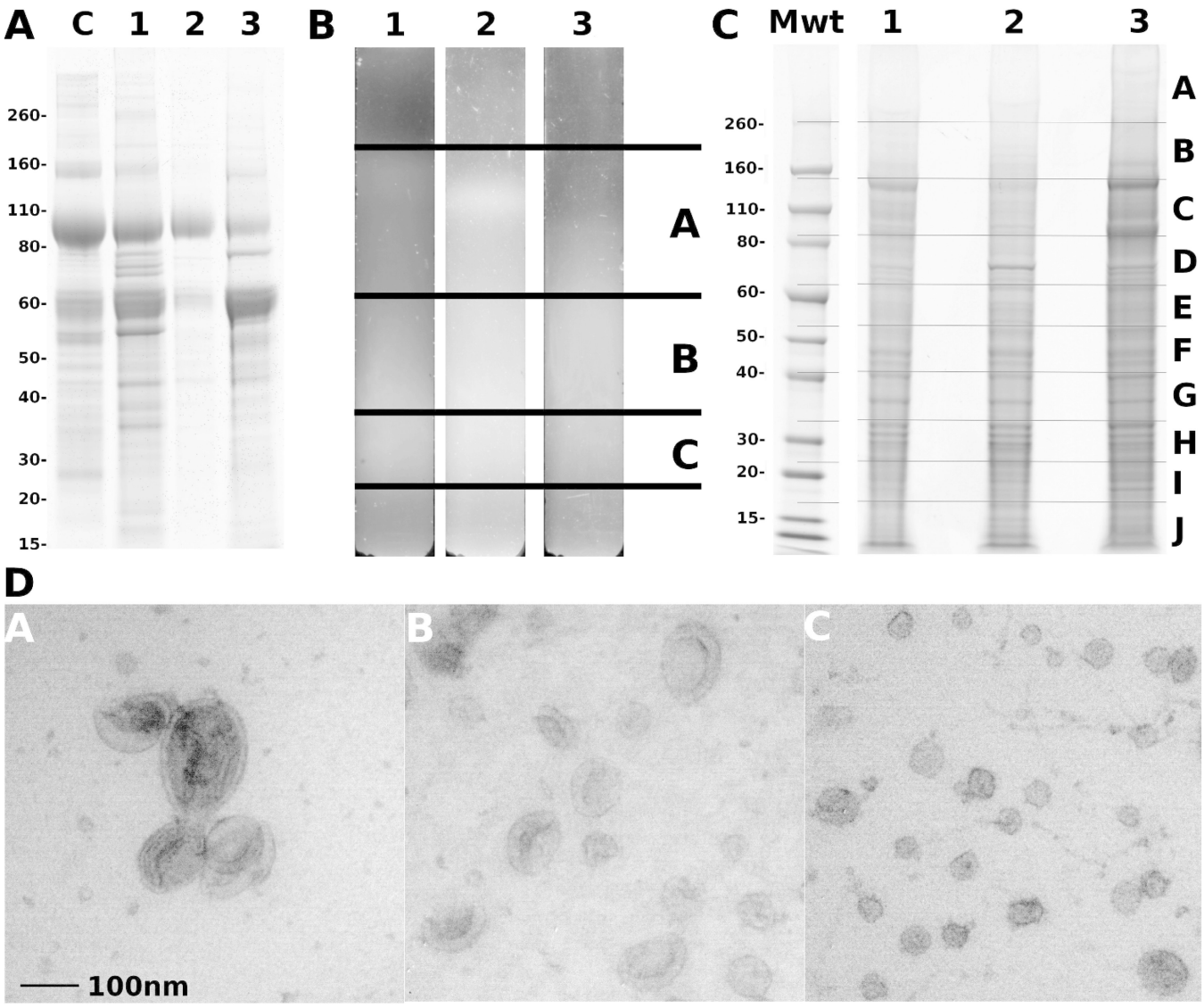


**Figure 6.**

GMVs from individuals with glomerular diseases: **6A** Crude exosomes from one normal (C) and three glomerular disease cases #1–3. THP resolves at 85–100kDa & albumin at 60–67kDa. Albumin mainly remains in solution under these conditions with only moderate enhancement in the nephrotic individuals. **6B** Transilluminated ultracentrifuge tubes with gradients obtained from cases with glomerular disease: .#1 and 2 resolved well whereas the #3 resolved less well defined bands, although we did not have any difficulty fractionating bands of interest in #3. **6C**: Pellets from $D_2O$ gradients SDS PAGE Coomassie brilliant blue stained prior to gel sectioning (#3 has a small contaminating THP band at 85kDa). **6D**: Representative TEM of ELVs from individual #1, fractions A, B and C.

## Table 1

Clinical characteristics of patients with glomerular disease in this study.

| | Case #1 | Case #2 | Case #3 |
|---|---|---|---|
| **Age** | 41 | 73 | 69 |
| **Gender** | Female | Male | Male |
| **Renal pathology** | Membranous nephropathy | Membranoproliferative glomerulonephritis ($IgG_3$ isotype) | Membranous nephropathy |
| **Proteinuria** | 4.7g/24 hours | 4.6g/24 hours | 1.8g/24 hours |
| **Serum Creatinine** | 0.6mg/dL | 2.5mg/dL | 1.2mg/dL |
| **eGFR** | >60ml/min | 42ml/min/SA[¥] | 60ml/min |
| **Treatment** | Losartan 100mg/d<br>Furosemide 40mg /d | CyBorD protocol[*] cycle 1<br>Amlodipine 5mg/d<br>Bumetanide 0.5 mg qod<br>Metoprolol succinate 25 mg/d<br>Lisinopril/HCTZ 30–37.5 mg /d | Lisinopril 40mg/d<br>Metoprolol succinate 25 mg/d |
| **Proteins identified** | 3258 | 3197 | 4189 |

[*] CyBorD protocol: 150 mg/$m^2$ of cyclophosphamide po once weekly(dose reduced for renal function and age), 20 mg of dexamethasone po once weekly, 3 mg (1.5 mg/$m^2$) of subcutaneous bortezomib once weekly. Each cycle consisted of four treatments, usually 3–6 cycles.

[¥] Measured by 24 hour urine creatinine clearance.

**Table 2**

**Proteomic analysis of GMVs reveals enrichment for many known inherited glomerular disease and pathogenic proteins in acquired forms of glomerulonephritis**

List of selected glomerular proteins identified and peptide numbers identified in this study. Total peptide number in fraction C for each protein with percentage protein coverage (peptides are reported in supplemental table 2A).

| Glomerular Protein | Uniprot ID and SwissProt ID & Gene name | Peptides in Fraction C | Gel Section[a] | Protein Coverage (%) | Localization | Observed in Other Urine ELV studies | OMIM | Comments | Reference |
|---|---|---|---|---|---|---|---|---|---|
| Fibronectin 1 | FINC_HUMAN P02751 | 4 | A | 29 | Mesangial and subendothelial cells | 1 peptide NHLBI | 135600 | Extracellular matrix protein –AD fibronectin glomerulopathy | 57, 58 |
| Megalin | LRP2_HUMAN P98164 | 140 | A | 35 | Proximal tubule | 84 peptides NHLBI; Wang | 222448 139200 | Mutations cause AR Donnai-Barrow & facioocculoacousticorenal syndromes. Associated with proteinuria | 5960 |
| Cubilin | CUBN_HUMAN O60494 | 69 | A | 23 | Proximal tubule | 104 peptides NHLBI, Wang | - | 1 bp homozygous deletion led to NS in two siblings. Another mutation associated with IgA nephropathy. | 61, 62 |
| Complement C3 | CO3_HUMAN P01024 | 34 | A | 8 | GBM, mesangium, Capillary loops | 1 peptide NHLBI; Wang | 120700 | Mutated in atypical HUS (Dense deposit disease and membranoproliferative GN) subendothelial electron-dense deposits along the GBM | 63,64 |
| Complement factor B | CFAB_HUMAN P00751 | 4 | A | 7 | - | No | 138470 | Atypical HUS | 65 |
| Myosin 9 | MYH9_HUMAN P35579 | 56 | B | 35 | Podocyte Mesangial cells | 19 peptides NHLBI | 160775 | Fechtner & Epstein syndromes-AD disorders with macrothrombocytopenia and characteristic leukocyte inclusions, GN, deafness & cataracts. Myh9 podocyte deletion in C57BL/6 mice results in susceptibility to doxorubicin glomerulopathy. | 66, 67 |

| Glomerular Protein | Uniprot ID and SwissProt ID & Gene name | Peptides in Fraction C | Gel Section[a] | Protein Coverage (%) | Localization | Observed in Other Urine ELV studies | OMIM | Comments | Reference |
|---|---|---|---|---|---|---|---|---|---|
| PTPRO | Q8IYG3_HUMAN PTPRO,GLEPP1 | 2 | B | 3 | Podocyte | 2 peptides NHLBI | 600579 | AR childhood NS. Tyrosine phosphatase expressed at the apical podocyte foot process membranes & necessary for their maintenance. | 68, 69 |
| Human Leukocyte (neutrophil) elastase | ELNE_HUMAN ELANE P08246 | 9 | B | 5 | Glomerular endothelial cells | 2 peptides NHLBI; Wang | 130130 | ANCA Vasculitis; granular endothelial elastase deposits in glomerular endothelial cells and Bowman's capsule in crescentic GN | 70 |
| CD2AP | CD2AP_HUMAN Q9Y5K6 | 27 | D | 55 | Podocyte | 14 peptides NHLBI, Wang | 604241 | Hereditary and sporadic FSGS. Gatekeeper of the podocyte TGF-β response Adaptor protein involved in maintenance of the slit diaphragm. | 71, 72 |
| Complement Decay accelerating Factor (CD55) | DAF_HUMAN CD55 P08174 | 18 | D | 46 | Mesangial epithelial cells | Wang | 604241 | Accelerates the decay of C3 and C5 convertases, participating in classical and alternative complement activation pathways & involved in the pathogenesis of immune complex GN with nephritic–NS phenotype. | 73, 74 |
| Myeloperoxidase | PERM_HUMAN P05164 | 6 | E | 9 | Glomerular capillary | 2 peptides NHLBI | 606989 | Anti-apoptosis defense response hydrogen peroxide catabolism response to oxidative stress, antibacterial PMN protein. Implicated in renal vasculitis. | 75 |
| Podocin | PODO_HUMAN NPHS2 | 7 | F | 23 | Podocyte & slit diaphragm | 6 peptides NHLBI | 604241 | AR steroid resistant NS. | 76 |
| Apolipoprotein E | APOE_HUMAN P02649 | 13 | G | 55 | Mesangial | 6 peptides NHLBI | 611771 | Mutations cause lipoprotein glomerulpathy. | 77 |
| CD151 | CD151_HUMAN P48509 | 4 | H | 4 | Podocyte Podocyte-GBM interface | Wang | 609057 | Tetraspanin-24. AR hereditary nephritis sensorineural deafness, pretibial epidermolysis | 7879, 8081, 82 |

| Glomerular Protein | Uniprot ID and SwissProt ID & Gene name | Peptides in Fraction C | Gel Section[a] | Protein Coverage (%) | Localization | Observed in Other Urine ELV studies | OMIM | Comments | Reference |
|---|---|---|---|---|---|---|---|---|---|
| | | | | | | | | bullosa, & β-thalassemia minor. Essential for the proper a<br>-thalassemia minor. Essential for the proper assembly of t<br>-thalassemia minor. Essential for the proper assembly of t<br>-thalassemia minor. Essential for the proper assembly of t<br>-thalassemia minor. Essential for the proper assembly of t<br>-thalassemia minor. Essential for the proper assembly of t | |
| Integrin alpha 3 | ITA3_HUMAN P26006 | 5 | H | 5 | GBM | Wang | 614748 | AR congenital NS (FSGS), interstitial lung disease &skin fragility (epidermolysis bullosa). Glycosylation defects reported to prevent the biosynthesis of functional α3β integrin hetereodimer. | 8384 |
| Rho GDP-dissociation inhibitor 1 | GDIR_HUMAN P52565 | 13 | H | 72 | Podocyte | Wang NHLBI | 601925 | AR SRNS via defective RHO GTPase signaling | 85, 86 |
| Alpha actinin 4 | ACTN4_HUMAN O43707 | 50 | I | 68 | Podocyte | Wang | 603278 | AD FSGS. Actin binding & crosslinking protein probably involved in vesicular trafficking via its association with the CART complex (necessary for efficient transferrin receptor recycling). Also identified in our previous exosome study. | 10, 87, 88 |
| Cdc42 | CDC42_HUMAN P60953 | 11 | I | 63 | Podocyte | 2 peptides NHLBI | 116952 | AD FSGS. Charcot-Marie-Tooth disease with glomerulpathy (FSGS). Required for actin polymerization after clustering of nephrin and leads to congenital NS& renal failure in Nphs $^{-/-}$ Cdc 42 $^{flx/flx}$ mice. | 89 |
| Cofilin-1 | COF1_HUMAN P23528 | 15 | I | 76 | Podocyte | 5 peptides NHLBI;Wang | 270400 | Renal hypoplasia. Knockdown compromised glomerular filtration & podocyte effacement in zebrafish. Cofilin-1 is the dominant isoform. | 90 |

*Kidney Int*. Author manuscript; available in PMC 2014 November 01.

| Glomerular Protein | Uniprot ID and SwissProt ID & Gene name | Peptides in Fraction C | Gel Section[a] | Protein Coverage (%) | Localization | Observed in Other Urine ELV studies | OMIM | Comments | Reference |
|---|---|---|---|---|---|---|---|---|---|
| Myosin 1E | MYO1E_HUMAN Q12965 | 5 | J | 5 | Podocyte | Wang | 614131 | AR FSGS/ NS. Localized to lamellopodia tips. Disruption promotes podocyte injury, thickening & disorganization of GBM. | 4, 8891–93 |

mDias and Integrin B4 were absent. Annexin family COLVA1; COL15A1 were present.

[*] Gel section with highest abundance.

GN= Glomerulonephritis. FSGS: Focal segmental glomerulosclerosis. aHUS- Atypical hemolytic uremic syndrome. NS- Nephrotic syndrome. AR- Autosomal recessive. AD- Autosomal dominant. GBM: glomerular basement membrane.

Note: Wang *et al* do not provide peptide coverage data only spectral intensities.[15]

*Kidney Int*. Author manuscript; available in PMC 2014 November 01.

**Table 3**

GMVs are enriched for many proteins involved in glomerular biology.

| Glomerular Protein | Uniprot Swiss Prot ID | Gene Name | Coverage in Fraction C (%) | Peptide Count | Localization | Previously seen in ELVs | Comments | Reference |
|---|---|---|---|---|---|---|---|---|
| Podocalyxin | PODXL_HUMAN B7ZKQ8 | Podocalyxin-like | 25 | 12 | Podocyte | NHLBI | Abundant protein in GMVs. Creates negative charge on secondary podocyte foot processes. | 28, 29 |
| Lysosomal associated membrane protein 2 LAMP2 | LAMP2_HUMAN P13473 | LAMP2 | 14 | 5 | - | H, NHLBI | Proposed autoantigen role in pauciimmune glomerulonephritis and Henoch-Schönlein purpura. | 94, 95 |
| Src substrate cortactin | SRC8_HUMAN Q14247 | CTTN | 44 | 22 | Podocyte | | Mediates interaction between podocalyxin and actin filaments. Interacts with PODXL. | 96 |
| Rab 23 | SRC8_HUMAN Q9ULC3 | RAB23 | 47 | 9 | Podocyte | Hogan | Expressed in the glomerulus. | 97 |
| ENPP6 | ENPP6_HUMAN Q6UWR7 | ENPP6 | 53 | 17 | - | H, NHLBI | Known secreted protein; mechanism hitherto unknown. Candidate biomarker of rat diabetic nephropathy. | 4,98 |
| Ezrin | EZRI_HUMAN P15311 | EZR | 73 | 62 | Podocyte | Yes | Glomerular epithelial cell marker in glomerulogenesis. | 99 |
| Complement C4B | CO4B_HUMAN P0C0L5 | C4B | 4 | 6 | Glomerular capillary endothelial cells | W | Susceptibility to SLE. Complement C4 is made in vivo in glomerular capillary endothelium cells | 61,62 |
| Agrin | AGRIN_HUMAN O00468 | AGRN | 9 | 17 | GBM | No | Probable human glomerular permselectivity modulator. May anchor GBM to cytoskeleton. A major heparan sulfate proteoglycan. | 87, 88 |
| FAT4 | AGRIN_HUMAN Q6V0I7 | FAT4 | 0.8 | 2 | Podocyte | H | Fat 4 −/− mice have small kidneys and develop cystic disease. Expressed in glomeruli-involved in planar cell polarity. | 100 |
| CD59 | CD59_HUMAN P13987 | CD59 | 26 | 6 | - | W, NHLBI | Complement regulatory protein that inhibits the terminal part of the complement system-membrane attack complex (MAC). | 101 |
| Talin 1 | TLN1_HUMAN Q9Y490 | TLN1 | 8 | 14 | Glomerulus | W, NHLBI | Adaptor proteins that connect the integrin family of cell adhesion receptors to cytoskeletal actin. | 102 |

| Glomerular Protein | Uniprot Swiss Prot ID | Gene Name | Coverage in Fraction C (%) | Peptide Count | Localization | Previously seen in ELVs | Comments | Reference |
|---|---|---|---|---|---|---|---|---|
| Syntenin 1 | SDCB1_HUMAN O00560 | SDCBP | 86 | 38 | - | NHLBI | Adaptor protein in apical endocytic pathway-top ranked protein in our data by percentage coverage. | 103 |
| Neprilysin (neutral endopeptidase) | NEP_HUMAN P08473 | CD10 | 71 | 79 | Podocyte | W | Protease that cleaves ACE. Induces human membranous glomerulonephritis in neonates cases of membranous nephropathy in newborns from neutral endopeptidase-deficient mothers. | 104, 105 |
| Na(+)/H(+) exchange regulatory cofactor 2 | NHRF2_HUMAN Q15599 | SLC9A3R2 | 14 | 3 | Podocyte | NHLBI (1 peptide) | Podocyte cytoskeleton connects to podocalyxin through this protein. | 106 |
| Angiotensin-converting enzyme 2 | ACE2_HUMAN Q9BYF1 | ACE2 | 30 | 19 | Podocyte | NHLBI | Present in podocyte foot processes. | 107, 108 |
| Angiotensin-converting enzyme | ACE_HUMAN P12821 | ACE | 72 | 54 | Endothelial cells | NHLBI | Traverses from capillary endothelial cells to podocytes. | 108 |

Peptide count is for fraction C. W; Wang proteome[15]. H- Hogan 2009 proteome.[10] NHLBI- NHLBI urine exosome database[4,13].